A Modified 4×4 Butler Matrix Based Switched Beamforming Network with Five Beams

Qutaibah Khaled Al-Marwan

Submitted to the
Institute of Graduate Studies and Research
in partial fulfilment of the requirements for the degree of

Master of Science
in
Electrical and Electronic Engineering

Eastern Mediterranean University
February 2017
Gazimağusa, North Cyprus

Approval of the Institute of Graduate Studies and Research

Prof. Dr. Mustafa Tümer
Director

I certify that this thesis satisfies the requirements as a thesis for the degree of Master of Science in Electrical and Electronic Engineering.

Prof. Dr. Hasan Demirel
Chair, Department of Electrical and Electronic Engineering

We certify that we have read this thesis and that in our opinion it is fully adequate in scope and quality as a thesis for the degree of Master of Science in Electrical and Electronic Engineering.

Asst. Prof. Dr. Rasime Uyguroğlu
Supervisor

Examining Committee

1. Prof. Dr. Hasan Demirel
2. Prof. Dr. Abdullah Öztoprak
3. Asst. Prof. Dr. Rasime Uyguroğlu

ABSTRACT

In this work 4x4 Butler matrix with 1×4 microstrip patch antenna array has been proposed to form a switched beamforming network operating at 3 GHz. This beamformer generates 4 orthogonal beams.

4x4 Butler matrix comprises 4 directional couplers, two phase shifters and two crossovers. The directional couplers have been used to divide the power equally with 90° phase shift, the phase shifters performs the phase delay in the design and the crossover works for isolation. All simulation results of these components matched the theory.

Linear 1×4 microstrip patch antenna array elements have been matched using inset feed technique. These elements had a good performance at the design frequency.

The CST MICROWAVE STUDIO SUIT was used for simulations. The total size of the Butler matrix is 104 mm×100mm. The return loss obtained was less than –15 dB and the output power distribution was in the range of -6 to -8 dB at the 3GHz design frequency. The four beams have been obtained in the directions -14°, -42°, 42° and 14° with a narrow beamwidth and with a gain of 11.4 dB, 11.2 dB, 11.2dB, and 11.4dB respectively

A modified Butler matrix also has been proposed to generate a fifth beam at together with the original four beams obtained in the conventional design. The modification increased the scan capability

Keywords: 4x4 Butler matrix, beamforming, linear array, radiation pattern.

ÖZ

Bu çalışmada, 3 GHz frekansında 1x4 mikro şerit yama anten dizili, anahtarlamalı hüzme oluşturma ağı olan bir 4x4 Butler matrisi önerilmiştir. Bu hüzme oluşturucu, 4 dik hüzme üretmektedir.

4x4 Butler matrisi 4 yönlü birleştirici, iki faz kaydırıcı ve iki geçitten oluşmaktadır. Yönlü birleştiriciler, gücü 90˚ faz kayması ile eşit olarak bölmek, faz kaydırıcılar tasarımda faz gecikmesi gerçekleştirmek ve geçitler de izolasyon sağlamak için kullanılmıştır. Bu tasarımdan elde edilen sonuçlar teori ile uyum içerisindedir.

1×4 Mikro şerit yama anten dizi elemanları, içe besleme tekniği kullanılarak uyumlaştırılmıştır. Bu elemanlar tasarım frekansında iyi performans göstermiştir.

Çalışma Mikrodalga CST benzetim yazılımı kullanılarak gerçekleştirilmiştir. Butler matrisinin boyutları 104 mm × 100 mm'dir. 3GHz tasarım frekansında elde edilen dönüş kaybı -15 dB'den az, çıkış gücü dağılımı ise -6 ila -8 dB aralığındadır. -14 °, -42 °, 42 ° ve 14 ° yönlerinde, sırasıyla 11.4 dB, 11.2 dB, 11.2dB ve 11.4dB kazancı olan dar hüzme genişliğine sahip dört hüzme elde edilmiştir.

Geleneksel Butler matris tasarımında değişiklik yapılarak, elde edilen dört hüzmeye ek olarak 0° yönünde beşinci bir hüzme elde edilmiş ve tarama kapasitesi artırılmıştır.

Anahtar Kelimeler: Butler matrisi, hüzme oluşturma, doğrusal dizi, radayassyon deseni

DEDICATION

To My Family

ACKNOWLEDGMENT

First and above all, I praise God, the almighty for providing me this opportunity and granting me the capability to proceed successfully.

I must extend my sincere gratitude to my dissertation advisor Asst. Prof. Dr. Rasime Uyguroğlu whose professional guidance, valuable advice, and feedback have shaped my ideas and position and pushed me and my research much further than I have expected. I would also like to extend my thanks to the other members of the committee, Prof. Dr. Abdullah Öztoprak and Prof. Dr. Hasan Demirel for their encouragement and support during my years of study to accomplish this work.

As very few know, there is much sacrifice when studying and researching, and defending a dissertation. Therefore, I am indebted to my father, Khaled Al-Omari, my mother, Huda Al-Omari and my uncle Khaliefah Al-Omari whom I also dedicate this project to for their love, tolerance, and support through the two years of study.

Next, to acknowledge my siblings (Abdullah, Dr.Nusaibah, Najah, Mohammad, Manal, Saleh, Hassan, Ibraheem, Areej, Hadieh, Shahla, Ghadeer, Laith, Ahmad, Yaman, Ghena, Rand, Baisan, Qais, Taj, Tamara, Dalal, Aya and Um Fakher) would not credit them enough. Their support does not stop at this momentous achievement. They have a great deal in shaping the man and the scholar I am now. I am so proud to be their brother and I was, am, will always be indebted to their love and support.

I would like to thank my uncle's family (Amneh ,Amal, Mohammad, Ahmad and Tahsein) and their families, I also want to extend my gratitude to my friends Hasan ,Baraa, Bassam, Mohammad, Moataz, Ali, Abu Saif, Abudallah, Mamoon, Yazan Mohammad Harastani, Samer, Abudurahman, Fakher, Majd, Khaled, Rayan and Mohammad Alquraan) for their belief in me and for their prayers and love words that encouraged me to finish this project.

Special thank for my third brother Alaelldien for his support and his known sentence (everything will be very well).

I want to express my sincere gratitude to my friend whom I consider a sister of me. Dr.Aya Akkawi for her faith in me as a scholar who still encourages me to pursue my PhD study. Her support and prayers.

Finally, I would express my thanks again to my friend whom I consider a copy of me my little brother Saleh for his love words, his enthusiasm in what I am doing, and his faith in me as a scholar. His inspiration, love, support, and prayers are tremendous and there are no words to credit his enough.

TABLE OF CONTENTS

LIST OF TABLES

LIST OF FIGURES

LIST OF SYMBOLS AND ABBREVIATIONS

ASA	Adaptive Smart Antenna
BM	Butler Matrix
c	Speed of light
CST	Computer simulation technology
DOA	Direction of Arrival
DSP	Digital Signal Processor
EM	Electromagnetic
ESA	Electronically Scanned Array
f_r	Resonant frequency
FR-4	Flame Retardant 4
h	Height
HPBW	Half Power Beamwidth
IEEE	Institute of Electrical and Electronics Engineers
L	Length
S_{ij}	Scattering matrix element
SBS	Switched-beam Systems
SIR	Signal-to-Interference Ratio
SLL	Sidelobe Level
TEM	Transverse electromagnetic
W	Width
Z	Impedance
ε_r	Relative permittivity
ε_{reff}	Effective relative permittivity

λ_0	Free space wavelength
λ_g	Wavelength of propagation

Chapter 1

INTRODUCTION

1.1 Introduction

Nowadays, the performance of wireless communication systems has improved by the use of smart antennas [1], which leads us to predict that the wireless revolution will get significant impact in future [2].

1.2 Antenna Array Overview

We use antenna arrays to obtain a narrow concentrated beam with a small radiation effect in other directions. Antenna array is a group of more than one identical element. As it is known, narrow beam is very important in wireless communication with many advantages, such as steerable beam capability and it’s high gain. Each element of an antenna array will radiate for long distances, known as far-field region so that we can achieve a signal that is not possible to be obtained by using a single element [3], [4].

1.2.1 Configuration of Antenna Array

An antenna array has many configurations that can be used in the design depending upon the application. The most common configurations are the linear and the circular arrays. There are other configurations of the antenna arrays such as conformal arrays as well.

1.3 Phased Array Antenna

In order to figure out the beamforming and smart antenna systems, we have to understand the concept of phased array antenna.

In a phased array the signal transmits (or receives) on different directions, then they are combined to obtain the output signal, this process is called beamforming [4]. As we can see in Figure 1.1 we have antenna elements that are separated by a distance **d** and **θ** is the angle between the incident wave and the normal direction if we consider the receiving mode; it will be the angle between the direction of the travelling wave and the normal direction if we consider the transmitting mode [3].

Referring to properties of the phased array antenna we can see the following application areas:

1. Radar for military use
2. Aircraft radar
3. Radio astronomy

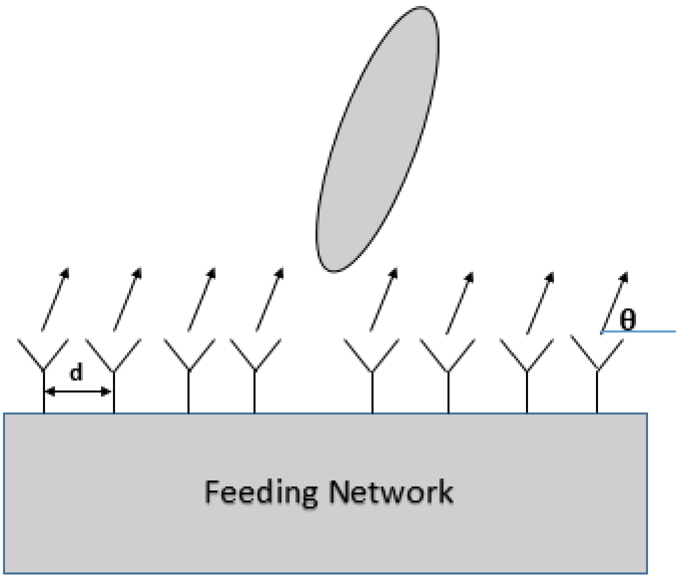

Figure 1.1: Block Diagram of the Phased Array

1.4 Beam Steering

In an antenna array, we can change the direction of the beam by moving the array mechanically to scan the coverage area. The mechanical movement is one of the methods to achieve beam steering, but we can get beam steering electronically by controlling the signal before combination by phase shifters. An electronic beam steering is also called beamforming [4].

1.5 Smart Antenna Systems

The main idea of the smart antenna system is spatial processing; the purpose of smart antenna gives us solutions for increasing the area covered and raising the higher transmission quality. The smart antenna is deployed to overcome interference and delay which occurs for our desired signal.

How does a smart antenna system work? If we have two antennas and DSP, the system receives a signal, DSP can determine the time delays from each antenna to estimate the direction of arrival (DOA) for producing a radiation pattern as shown in Figure 1.2 [4],[5].

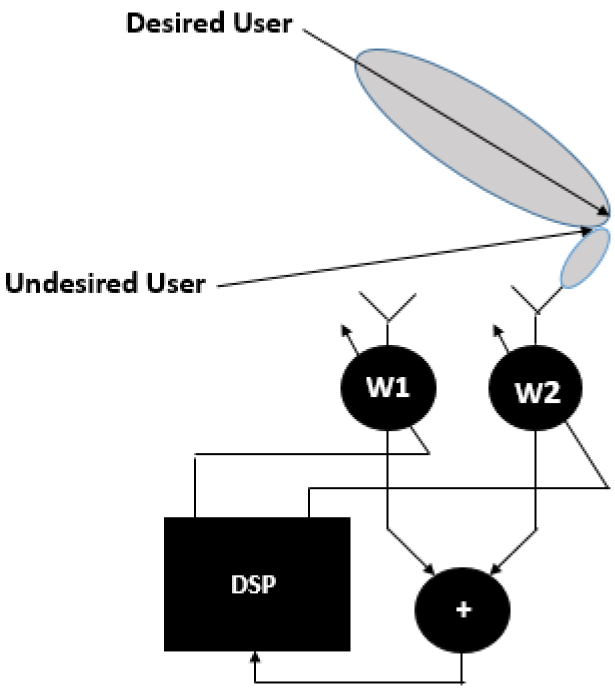

Figure 1.2: Principle of Smart Antenna System

1.5.1 Categories of Smart Antenna Systems

Smart antenna systems can be categorised into:

1. Switched-beam systems (SBS): The array pattern is changed dynamically and the system generates fixed, multiple and simultaneous beams, then the system using switching function will choose the appropriate switching technique [6]. The SBS principle is demonstrated in Figure 1.3(a).
2. Adaptive smart antenna (ASA): Adaptive array processors apply weight vector on the signal (see Figure 1.3(b)), and the signal will be controlled depends on the phase between the antenna elements. Only one beam pattern is produced and directed to the desired user [4]. ASA uses advanced signal processing more than SBS then it provides more intelligent operation [7].

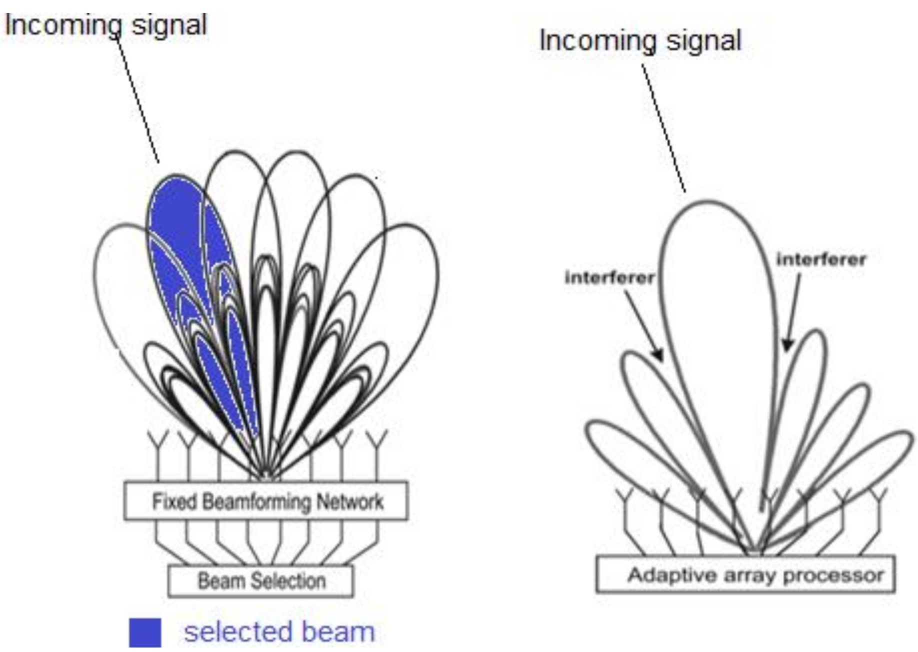

(a) Switched-Beam System, (b) Adaptive Array System.
Figure 1.3: Category of Smart Antenna System

1.5.2 Advantages and Disadvantages of Smart Antenna Systems

In smart antenna systems, the beam will be focused on the desired user instead of radiating in all directions compared with omnidirectional antennas, because the beam will not be radiated to an unwanted direction. In addition, the smart antenna has a low level of interference, and a low signal-to-interference ratio (SIR). On the other hand, there are many disadvantages for smart antenna systems; in a mobile system smart-antenna station, the transceiver is more complex than the transceiver used in the traditional base station. Each element array needs a transceiver [4].

1.6 Butler Matrix

In an Electronically Scanned Array (ESA) the beamforming network can be considered as the most important part [6]. It is also called a feeding network as it is feeding the antenna array by suitable amplitude and phase to form the radiation beams.There are many types of beamforming networks (beamformers) such as Mixer matrix, Blass matrix and Butler matrix [6-9]. Among of all feeding networks, the most commonly used is the Butler matrix (BM) because it is easy to fabricate [9], have a fewer number of components compared to other feeding networks and it has low cost.

For phased array, the Butler matrix has 2^n input and 2^n output. This matrix named $2^n \times 2^n$ or N×N Butler matrix where N=2^n and n>0. N orthogonal beams will be produced by N×N matrix. The coverage area by butler matrix is 0 to 360 degrees, which depends on the type of the element antennas and spacing between them [10].

Butler matrix has $\frac{N}{2}\times\log_2 N$ hybrids and $\frac{N}{2}\times\log_2 N - 1$ phase shifters to achieve the desired beams [7]. Figure 2.7 illustrates 4×4 Butler matrix, as it is shown it comprises two 45^{o} phase shifters, four hybrid 90^{o} couplers and two crossovers.

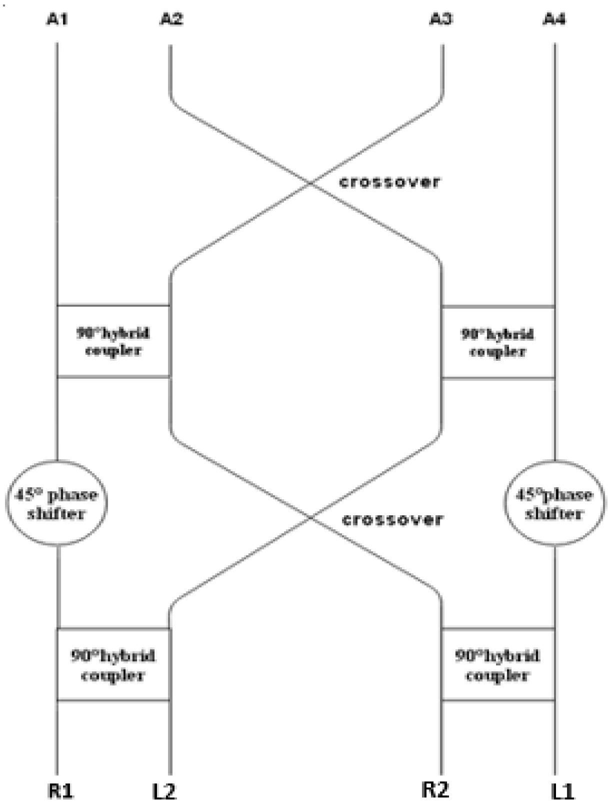

Figure 1.4: Block diagram of 4×4 Butler Matrix

As we see in the figure above 4×4 butler matrix has 4 inputs and 4 outputs, these four outputs will be inputs for the radiation elements to obtain four orthogonal beams. The phase differences ***β*** made by butler matrix give an ability to steer the beam to a certain direction [7]. The phase difference between the inputs of 4×4 Butler matrix and its outputs depending on the selected input port can be explained and summarised in the following matrix [8], [11]:

$$\begin{bmatrix} R2 \\ L1 \\ R1 \\ L2 \end{bmatrix} = \begin{bmatrix} 0 & -135 & 90 & -45 \\ 0 & -45 & -90 & -135 \\ 0 & 45 & 90 & 135 \\ 0 & 135 & -90 & 45 \end{bmatrix} \begin{bmatrix} A1 \\ A2 \\ A3 \\ A4 \end{bmatrix} \tag{1.1}$$

The phase difference between the input and output can be understandable from the previous matrix and Figure 1.4. For example if port R1 has been excited the phase difference between R1 and A1 is 0^o and between R1 and A1 is -45^o and so on.

Butler matrix takes the same behaviour when it transmits and receives, so it is considered a passive reciprocal network [11]. Butler matrix is used widely in smart antenna technologies especially in the cellular systems because it generates a narrow beam and high directivity [12].

1.7 Organization of this Work

Chapter 1, introduces the main concepts and basic definitions regarding Butler matrix and its applications, it mainly discusses antenna array, phased array and smart antenna system. Chapter 2 covers most commonly used Butler matrix types and some methods to reduce SSL which is considered as the main problem in Butler matrix.

Chapter 3, discusses the main theories regarding microstrip patch antenna and some of microwave circuits such as a directional coupler, crossover and phase shifter. Chapter 4, is about the design of components and combination of them in the form of 4×4 Butler matrix. Also includes the improvement of the directivity using the power divider. Chapter 5, discusses the results that have been obtained in Chapter 4.

Chapter 2

LITERATURE REVIEW

2.1 Introduction

Butler matrix is considered as one of the most commonly used beamforming network [10], which has been widely used in smart antenna systems, because it has many advantages as mentioned in Chapter 1. On the other hand there are some disadvantages that will be discussed in this chapter. The modified versions of the Butler matrix with the improvements will be included.

2.2 Butler Matrix

Butler matrix was introduced by J. Butler and R. Lowe [13] in 1961. It has been developed and studied till nowadays. It was improved by many antenna engineers and adopted to the new technology used in communication systems.

Kaifas, T. N et al have used Butler matrix in base station and mobile systems. 4×4 and 8×8 wide-band Butler matrix using elliptical coupler and using Lange coupler as a crossover were presented to cover 1.8-2.2 GHz [10].

In [12] 4×4 Butler matrix as a hybrid system with adaptive array has been presented by Siachalou, E et al.

Konstantinos et al used 8×8 Butler matrix with neural network to estimate the direction of arrivals by using microstrip antenna with inset line feeding [1].

Denindni et al have presented wide band 4×4 Butler matrix to cover 1.9-2.2 GHz, the interference problem was reduced and the broadband cross over increased the bandwidth [14].

Moubadir et al designed a microstrip antenna array with 8×8 Butler matrix to operate at 2.4 GHz, the square truncated and an edge-fed design was used to design the patch array [15].

Sahu et al designed 4×4 Butler matrix by branch-line coupler and cutting the ground plane to design the crossover. A significant size reduction has been obtained. The size of 4×4 Butler matrix was 40×40 mm [11].

Li et al proposed N×2N Butler matrix design. The number of radiation elements used was duplicated to reduce the side lobes level. The output ports of butler matrix were connected to 180° power divider for this purpose [13].

Fakoukakis et al reduced the side lobe levels by Butler-Like Matrix, the design has unequal Wilkinson power divider to obtain tapered output amplitude distribution [16].

Wincza et al designed 4×6 Butler matrix to reduce the side lobe level using compensating phase shifter and power splitters [17].

Chapter 3

MICROSTRIP ANTENNA AND MICROWAVE CIRCUITS

3.1 Introduction

An open guiding structure is a microstrip, and can be used as transmission line, in the manufacture and structure of microwave circuits such as couplers, crossovers and power dividers. Microstrip is also used in the construction of an antenna to produce microstrip antennas (patch antennas) [18]. Microstrip antennas and microwave components will be discussed in this chapter.

3.2 Microstrip Antennas

Microstrip antennas are considered of the most popular antennas currently being used, because of their general characteristics: they have lightweight, low cost, ease to fabricate and low profile [1]. The microstrip antenna comprises a substrate material, sandwiched on the bottom by a ground plane and on the top by a metallic strip (conducting patch). The configuration is shown in Figure 3.1.

Figure 3.1: Microstrip Antenna Structure

To be effective the metallic patch has to be very thin (h<<λ_0) where $\boldsymbol{\lambda_0}$ is the wave length in the free space, the ground plane has the same characteristics as that of the patch and it is separated from the patch by dielectric substrate, which has thickness (0.003 λ_0<< h<<0.005λ_0) and dielectric constant of ($2 \leq \epsilon_r \leq 12$). The selection of substrate depends upon the application of antenna and on its desired parameters. For example, thick substrate with low dielectric constant is the best choice for antenna radiation, but thin dielectric with high dielectric constant is appropriate within microwave circuits because that leads us to minimize radiation pattern and size of the circuit [4], [19].

The radiation patch could be formed in many shapes that can be mathematically expressed (rectangular, circular....etc.). Most commonly used model is the circular patch because it is easier to analyze and fabricate [4]. Dipole (thin strip) is very good to be used as a patch because it can take a small size in addition, to improve the bandwidth of the antenna [20].

3.2.1 Microstrip Feeding

In order to obtain the desired parameters of a microstrip antenna, we have to feed the antenna by one of the feeding techniques. The feeding techniques that are commonly used in microstrip antennas can be one of the following techniques [4]:

1. Microstrip line.
2. Coaxial probe.
3. Aperture coupling.
4. Proximity coupling.

3.2.1.1 Microstrip Line

By using this feeding technique, the connection between the patch antenna and the microstrip line will be direct. The width of line will be smaller than the width of the patch as it is shown in Figure 3.2. In this technique the structure is coplanar because the patch and the feeding line are on the same plane [21]. This technique is considered as the most commonly used feeding technique because it is ease of design characteristics [4].

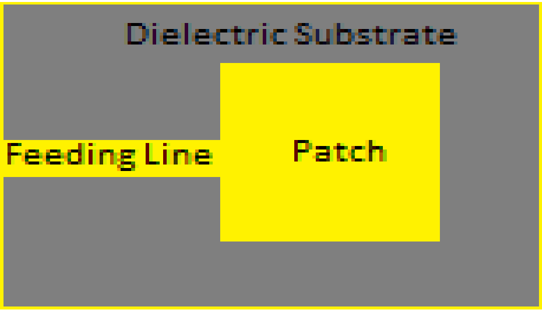

Figure 3.2: Microstrip Antenna with Feed Line

In this technique, the impedance of microstrip line is not the same as that of the patch, so that we have to perform some of matching techniques to match the feed line to the antenna [4].

3.2.1.2 Coaxial Probe

The coaxial cable has two conductors (inner, outer). In this feeding method the inner conductor passes from ground plane to patch plane on the other side of the antenna, crossing the substrate, while the outer connector of the coaxial cable is connected to the ground as shown in Figure 3.3.

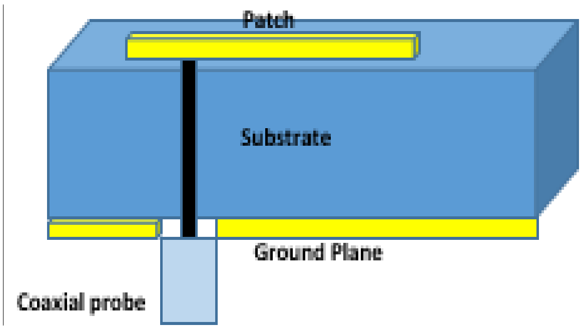

Figure 3.3: Coaxial Probe Feeding Method

Coaxial line can be located anywhere on the antenna, so that we can adjust the position of the line to obtain matching. This method is easy to fabricate and has low spurious radiation [21].

3.2.1.3 Aperture Coupling

As illustrated in Figure 3.4, two substrates are used in this configuration; they have the same ground plane located between them. The feed line is located on one of the two substrates and the patch will be printed on the top of other substrate. In this technique the feeding coupling occurs from the slot which is located in this common ground.

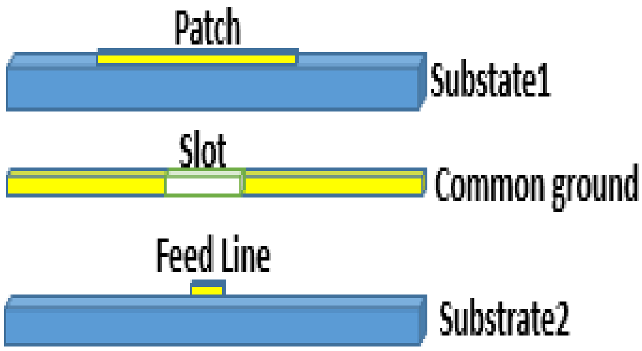

Figure 3.4: Microstrip Feeding Using Aperture Coupling Method.

The selected substrates depending on the feed and function of radiation, such as the feed substrate has to be very thin with a high dielectric constant, but another substrate could be thick with a low dielectric constant, as was mentioned earlier. This method of feeding has the widest range of bandwidth among of all methods [22], [23].

3.2.1.3 Proximity Coupling

In this technique, we have two substrates. The patch is printed on the top of one of them and the ground is located on the bottom on the other one, Figure 3.5 illustrates this and shows the feed line between these substrates.

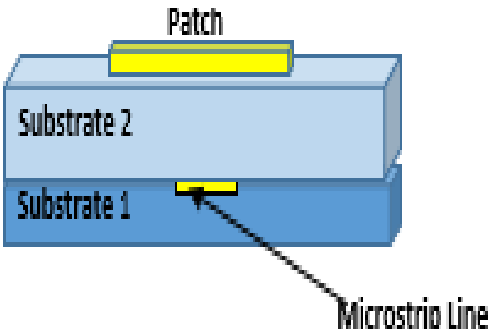

Figure 3.5: Proximity Coupling Feeding Method.

In this method, there is a capacitive coupling between the line and the patch which has to be taken into consideration in our design to obtain impedance matching. Using proximity coupling up to 13% bandwidth can be achieved by adjusting the terminated stub at the open end of the line. The substrate also can be selected to enhance the bandwidth of the antenna [24], [25].

3.2.2 Analysis and Design of Rectangular Microstrip

A transmission line, cavity and full wave models can be considered the most commonly used models for analysis of microstrip antenna [4]. In this work only the transmission line model was used; therefore we will only introduce this model.

3.2.2.1 Transmission Line Model

This analytical model can be considered as the simplest approach, but its accuracy is very low [4]. The antenna has been represented by two slots, each one has width W, height h and L the distance between them which is the length of the transmission line that separates them [26]. Figure 3.6 illustrates the idea of transmission line model. The microstrip line is located between two dielectrics, one of them is the substrate and another one the air as shown in Figure 3.7 (a). Figure 3.7 (b) illustrates the behavior of electrical field lines. As it is shown, most of them go in the substrate while some of them go through the air [27].

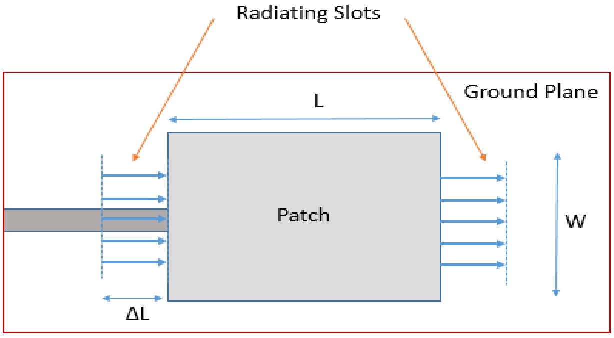

Figure 3.6: Transmission Line Model

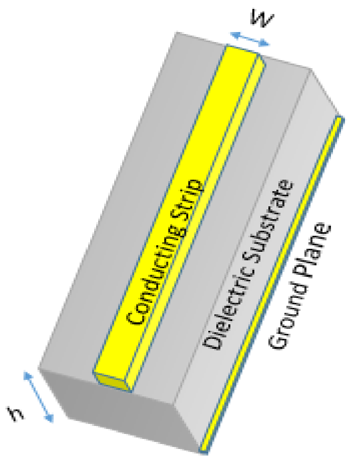

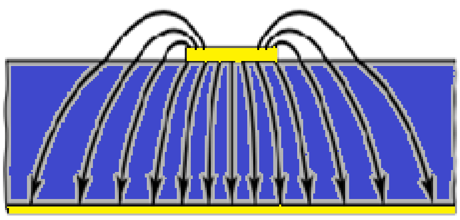

(a) (b)

Figure 3.7: (a) Structure of the Microstrip Line. (b) Distribution of Electrical Field.

For the line in Figure 3.7 we have to take the effective dielectric constant ϵ_{reff} into account because of the fringing and propagation in the line. ϵ_{reff} is in the range of $1 < \epsilon_{reff} < \epsilon_r$ which is given by [4].

$$\epsilon_{reff} = \frac{\epsilon_r + 1}{2} + \frac{\epsilon_r - 1}{2}\left[1 + 12\frac{h}{W}\right]^{-1/2} \tag{3.1}$$

where:

ϵ_r: Dielectric constant of the substrate.

h: The height of the substrate.

W: The line width.

Because of the difference in phase velocities between the air and the substrate, the pure transverse-electric-magnetic (TEM) mode could not be supported by the transmission line model, as this can support the quasi-TEM mode [28].

3.3 Microwave Components

3.3.1 Directional Coupler

Directional coupler can be considered as a passive microwave component, it is a four port network as shown in Figure 3. Power incident at port 1 will be divided between the through port (port 2) and the coupled port (port3), but no power will go through (port 4) which is the isolated port. In other word we can say that the power is coupled to port 3 [27].

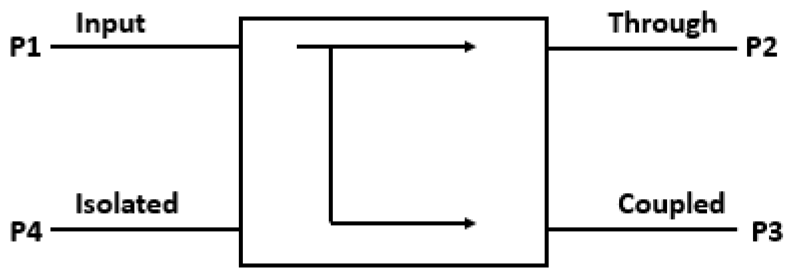

Figure 3.8: Block Diagram of a Directional Coupler

The power will be coupled to port 3 with coupling factor $\beta^2$and to port 2 with the coefficients α^2= 1- β^2. In the directional coupler, any port can be considered as an input port. For instance if port 2 is considered as the input port, then port 3 will be the isolated port, port 4 will be the coupled port and port 1 will be the through port [29].

The scattering matrix of the directional coupler is given by [29]:

$$[s] = \begin{bmatrix} 0 & S_{12} & S_{13} & S_{14} \\ S_{21} & 0 & S_{23} & S_{24} \\ S_{31} & S_{32} & 0 & S_{34} \\ S_{14} & S_{24} & S_{34} & 0 \end{bmatrix} \tag{3.2}$$

Note that S_{nm}= 0 where n=m, for having a lossless, matched and reciprocal directional coupler, the ten conditions which were mentioned in [29] have to be satisfied. To obtain this verification, the scattering matrix will be equation (3.3) for a symmetric coupler and equation (3.4) for an antisymmetric coupler.

$$[s] = \begin{bmatrix} 0 & \alpha & j\beta & 0 \\ \alpha & 0 & 0 & j\beta \\ j\beta & 0 & 0 & \alpha \\ 0 & j\beta & \alpha & 0 \end{bmatrix} \tag{3.3}$$

$$[s] = \begin{bmatrix} 0 & \alpha & j\beta & 0 \\ \alpha & 0 & 0 & -\beta \\ \beta & 0 & 0 & \alpha \\ 0 & -\beta & \alpha & 0 \end{bmatrix} \tag{3.4}$$

To specify the directional coupler, the following quantities have to be used [29]:

$$\text{Coupling} = C = 10 \log \frac{P1}{P2} = \text{-}20 \log \beta \text{ dB} \tag{3.3}$$

$$\text{Directivity} = D = 10 \log \frac{P3}{P4} = 20 \log \frac{\beta}{|S14|} \text{ Db} \tag{3.4}$$

$$\text{Isolation} = I = 10 \log \frac{P1}{P4} = 20 \log\lfloor S_{14} \rfloor \text{ dB} \tag{3.5}$$

$$\text{Insertion loss} = L = 10 \log \frac{P1}{P2} = 20 \log\lfloor S_{12} \rfloor \text{ dB} \tag{3.6}$$

According to the coupling factor C we can determine the value of α and β [29], [30].

3.3.1.1 The Quadrature Coupler (A 90° Hybrid coupler)

The quadrature (90°) hybrid coupler is considered a symmetric coupler. A 90° directional coupler has a 3dB coupling factor thus $\alpha = \beta = \frac{1}{\sqrt{2}}$ and will give phase shift of 90° between the two output signals [15], [29]. The 90° hybrid coupler scattering matrix will be expressed by [29]:

$$[S] = {}^{1}\!/\!_{\sqrt{2}} \begin{bmatrix} 0 & 1 & j & 0 \\ 1 & 0 & 0 & j \\ j & 0 & 0 & 1 \\ 0 & j & 1 & 0 \end{bmatrix} \tag{3.7}$$

In a 90° hybrid coupler the power will be divided equally between port 2 and port 3, and no power will go through port 4 as it was mentioned earlier. As shown in equation (3.7) the scattering matrix is symmetric$[S] = [S]^T$. So the input port can be considered any port, in which case the isolated port will be the port which is located on the same side as the input port, and the output ports will be on the other side [29]. The geometry of a branch line coupler can be shown in Figure 3.9.

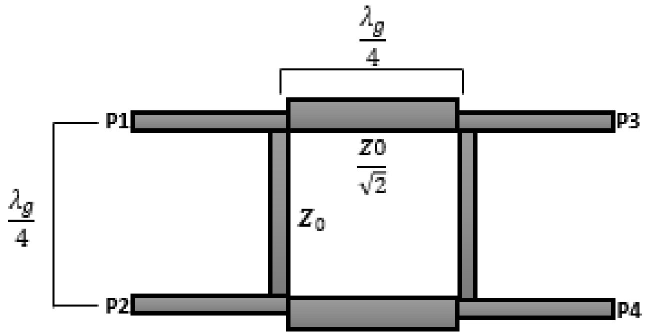

Figure 3.9: Layout of a Branch Line Coupler

As shown in Figure 3.9, a branch line coupler has four arms and are made by using stripline or microstrip line. Two of these arms are vertically parallel with $\lambda_g/4$ length and impedance $Z_0/\sqrt{2}$, and two arms are horizontally parallel with $\lambda_g/4$ length and Z_0

impedance, where Z_0 is the input impedance of the access port and $\lambda_g = \lambda/\sqrt{\epsilon_{reff}}$, λ is the wave length in the free space [29].

3.3.2 Crossover

Crossover is a four port network and is considered as one of the transmission line circuits, it is a result of cascading two branch line couplers to allow two signals to pass to the other side in the high degree of isolation as shown in Figure 3.10 and 3.11 [14], [31].

Figure 3.10: 0 dB Crossover Function

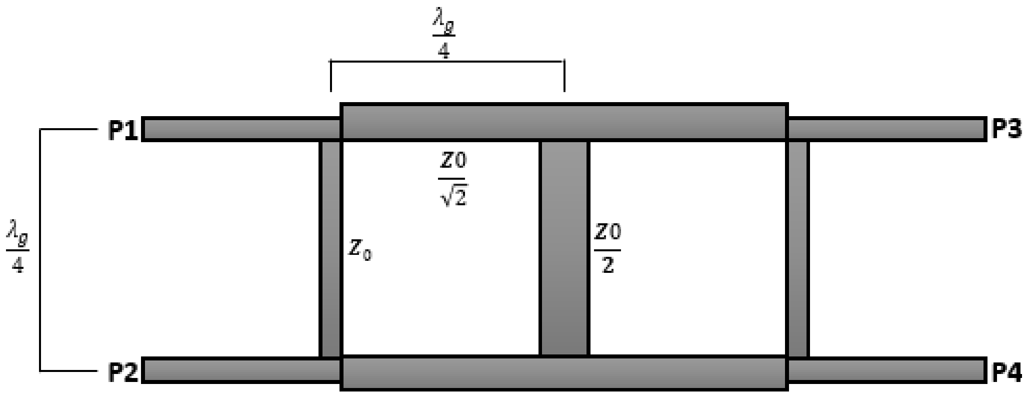

Figure 3.11: Layout of a 0 dB Crossover

The following matrix in equation (3.8) shows the scattering matrix of 0 dB crossover [32]:

$$[S] = \begin{bmatrix} 0 & 0 & j & 0 \\ 0 & 0 & 0 & j \\ j & 0 & 0 & 0 \\ 0 & j & 0 & 0 \end{bmatrix} \qquad 3.8$$

According to the scattering matrix $[S]$ and the Figures 3.10 and 3.11, we have four cases:

- The first case: If we suppose that the input port is port 1 then S_{11} ,S_{21} are and S_{41}equal to –infinity and S_{31}= 0 dB.
- The second case: If we have port 4 as an input port then S_{14}=S_{34}=S_{44}= -∞ dB and S_{24}= 0dB.
- The third case: If we consider port 2 as an input port S_{12}= S_{22}=S_{32}=-∞ and S_{42}=0dB.
- The fourth case: If our input is at port 3 then S_{23}=S_{33}=S_{43}= -∞ and S_{13}=0dB.

These cases can be achieved in the ideal case which implies perfect isolation.

3.3.3 Phase Shifter

The microstrip line and strip line are used to design the phased shifter, which is used to obtain a delay in the phase between two lines by adding extra length as shown in Figure 3.12 , the length of line 1 is more than the longer of line 2 by 2ΔL [15].

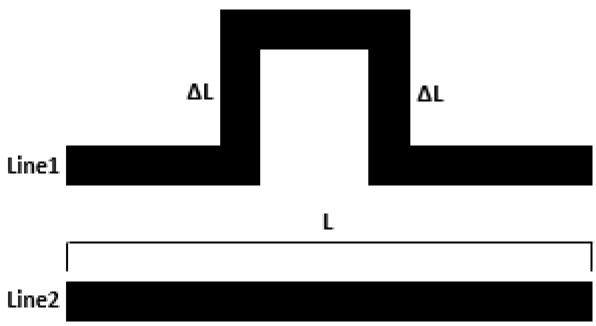

Figure 3.12: Phase Shifter

The phase shift is given by [32]:

$$\theta = \frac{2\pi\Delta L}{\lambda_g} \tag{3.9}$$

Where θ is the phase shift, ΔL is the extra length and λ_g is the wave length in the microstrip [15].

Chapter 4

DESIGN AND SIMULATION RESULTS

In This chapter we will show the process of designing hybrid coupler, crossover, phase shifter, a patch antenna and combine all of them to form a 4×4 Butler matrix. Note that all of these components have been simulated using CST STUDIO SUIT.

4.1 A 90° Hybrid Coupler (Branch Line Coupler)

As it is discussed in the previous chapter, a 90° hybrid coupler has four arms, each two parallel arms, having the same lengths and characteristic impedances as that shown in Figure 3.9. In our design, FR 4 has been used as a dielectric substrate with 1.6mm height and 4.4 dielectric constant. We have used microstrip line equations to obtain the dimensions of the coupler to operate at 3 GHz.

$$\boldsymbol{Z_0} = \begin{cases} \dfrac{60}{\epsilon_{reff}} \ln(8\dfrac{h}{W} + \dfrac{1}{8}\dfrac{W}{h}) & \dfrac{W}{h} \le 1 \\[2ex] \dfrac{120 \frac{\pi}{\epsilon_{reff}}}{\frac{W}{h} + 1.393 + .667\ \ln\left(\frac{W}{h} + 1.44\right)} & \dfrac{W}{h} \ge 1 \end{cases} \tag{4.1}$$

$$W = \begin{cases} \dfrac{8he^{A}}{e^{2A}} & \dfrac{W}{h} \le 2 \\[2ex] \dfrac{2h}{\pi}(B - 1 - \ln(\,2B - 1) + \dfrac{\epsilon_r - 1}{2\epsilon_r}\left(\ln(B-1) + .39 - \dfrac{0.61}{\epsilon_r}\right) & \dfrac{W}{h} \le 2 \end{cases} \tag{4.2}$$

$$A = \frac{Z_0}{60}\sqrt{\frac{\epsilon_r + 1}{2}} + \frac{\epsilon_r - 1}{\epsilon_r + 1}\ (\,0.23 + \frac{0.11}{\epsilon_r}) \tag{4.3}$$

$$B = \frac{377\pi}{2Z_0\sqrt{\epsilon_r}} \tag{4.4}$$

Using equations 4.1-4.4, we obtained the parameters of table 4.1.

Table4.1: Dimensions and Parameters of a 90° Hybrid Coupler

Parameters	Calculated	Optimized
$\boldsymbol{\lambda_g}$ **(50 Ω)**	54.799 mm	
$\boldsymbol{\lambda_g}$ **(35.355 Ω)**	53.559mm	
ε_{reff} **(50 Ω)**	3.33	
ε_{reff} **(35.355 Ω)**	3.486	
Length (50Ω)	13.699mm	12.8mm
Length (35.355 Ω)	13.38mm	12.3mm
Width (50 Ω)	3.059mm	3.00mm
Width (35.355 Ω)	5.228mm	4.6mm

After obtaining all the parameters of the design, the CST simulation software was used for simulations. Figures 4.1-4.5 show the design and simulation results of a 90° hybrid coupler in phase and amplitude.

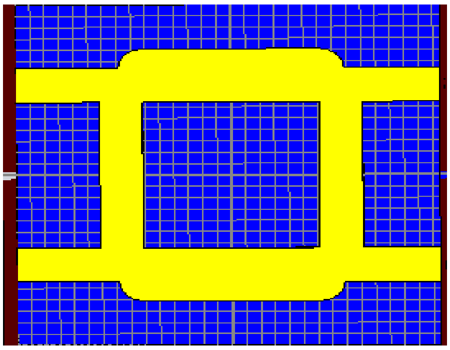

Figure 4.1: Layout of a 90° Directional coupler

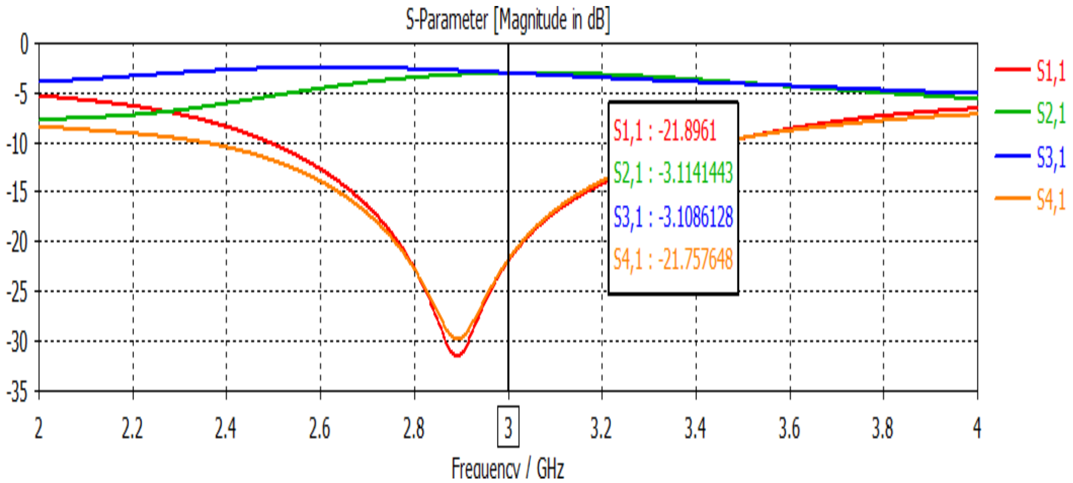

Figure 4.2: S-Parameters of a 90° Hybrid Coupler in dB (input port is port 1)

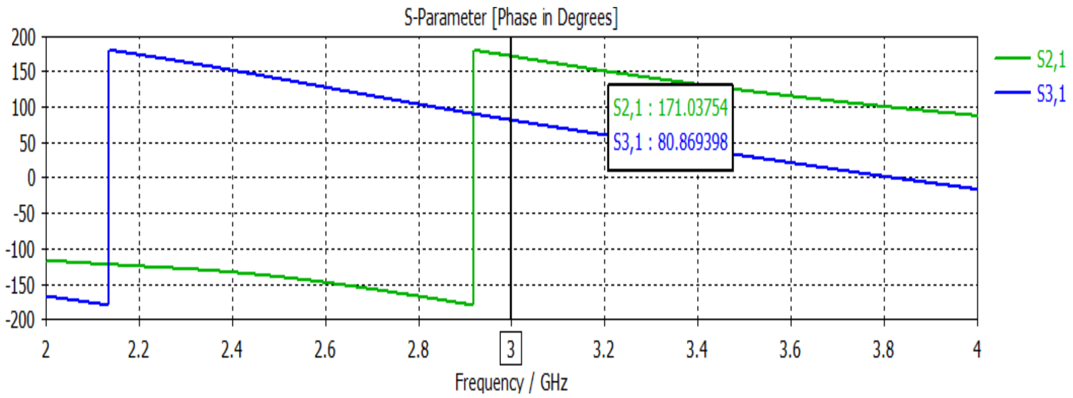

Figure 4.3: S-Parameters of a 90° Hybrid Coupler in Degree (input port is port 1)

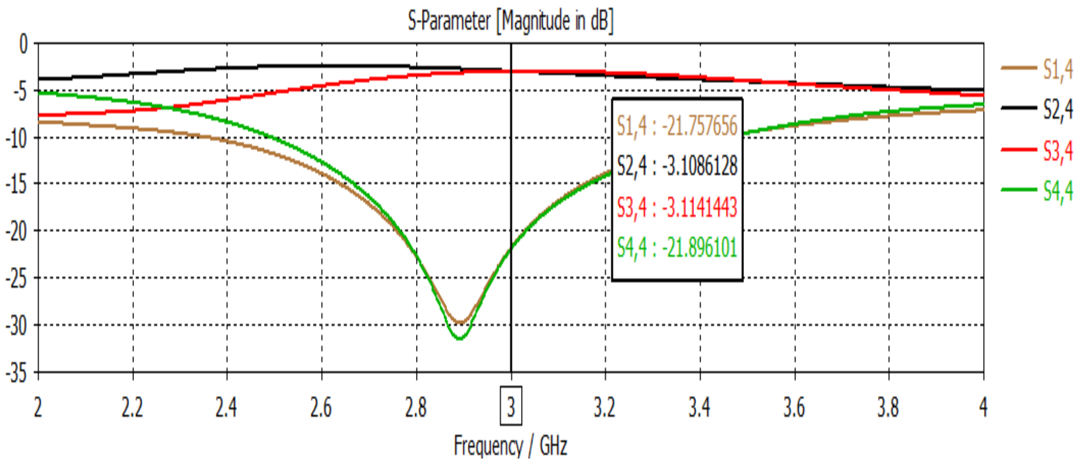

Figure 4.4: S-Parameters of a 90° Hybrid Coupler in dB (input port is port 4)

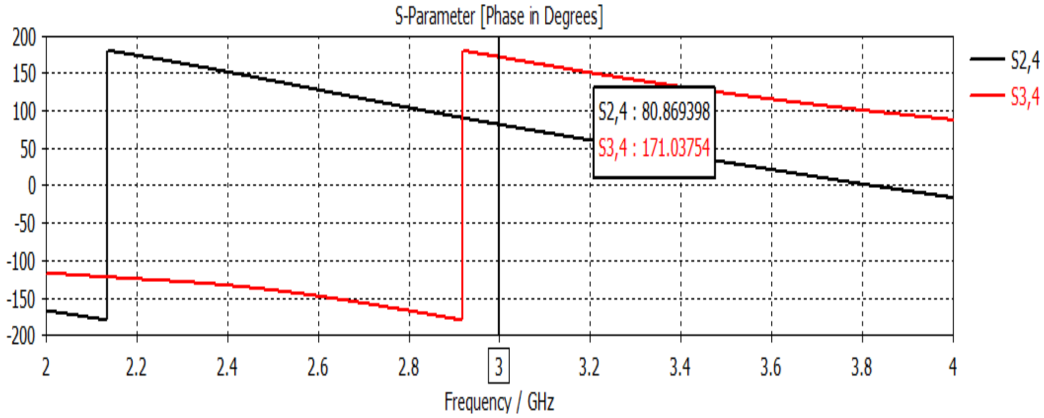

Figure 4.5: S-Parameters of a 90̊ Hybrid Coupler in degree (input port is port 4)

As was shown in Figures 4.2-4.5 (the input signal applied to port 1 and port 4) the results at 3 GHz frequency illustrate a good matching with the theory that was also described in chapter 3. The results have been summarized in Table 4.2 and 4.3.

Table 4.2: S-Parameter in Magnitude and Phase (input port 1)

Input port 1	Magnitude (dB)	Phase (degree)
S11	-21.8961	Irrelevant
S21	-3.1141	-171.0375
S31	-3.1086	80.8693
S41	-21.7576	Irrelevant

Table 4.3: S-Parameter in Magnitude and Phase (input port 4)

Input port 4	Magnitude (dB)	Phase (degree)
S14	-21.7576	Irrelevant
S24	-3.1086	80.8693
S34	-3.1141	-171.0375
S44	-21.8961	Irrelevant

In accordance with the previous results, we can say that a 90° hybrid coupler has been successfully designed to operate at the frequency of 3 GHz.

4.2 Crossover

After designing a 90° hybrid coupler, the design of the crossover will be easy because it is a cascading of two quadrature couplers, using the microstrip equations. We can obtain all parameters that will be used in the design of the crossover, which are listed in Table 4.4. In this design, we used FR-4 as a dielectric substrate (ε_r= 4.4 and h=1.6mm) and the frequency of operation has been chosen to be 3 GHz.

Table 4.4: Dimensions and Parameters of a Crossover

Parameters	Calculated	Optimized
λ_g (50 Ω)	54.799mm	
λ_g (35.355 Ω)	53.559mm	
λ_g(25 Ω)	52.628mm	
ε_{reff} (50 Ω)	3.33	
ε_{reff} (35.355 Ω)	3.486	
ε_{reff} (25 Ω)	3.633	
Length (50Ω)	13.699mm	12.8mm
Length (35.355 Ω)	26.74mm	24.6mm
Length (25 Ω)	13.157mm	12.8mm
Width (50 Ω)	3.059mm	3.00mm
Width (35.355 Ω)	5.228mm	4.6mm
Width (25 Ω)	8.28mm	7.95mm

Now these values have been used to design the crossover using CST STUDIO SUIT.

The design and the simulation results are shown in Figures 4.6-4.8.

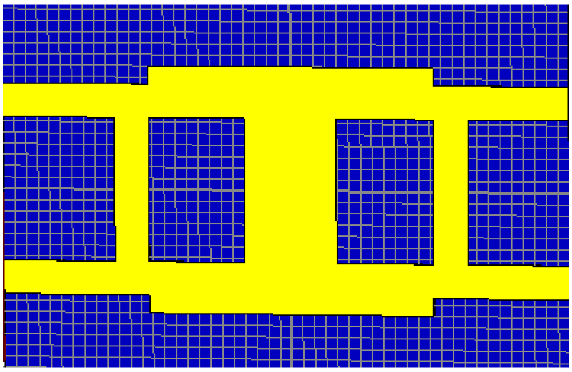

Figure 4.6: Layout of a 0 dB Crossover

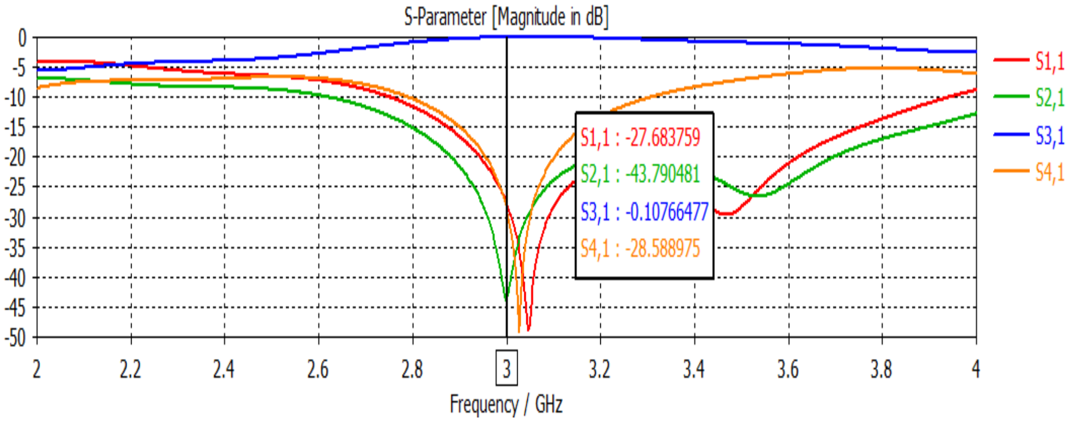

Figure 4.7: S-Parameters of a 0 dB Crossover (input port1)

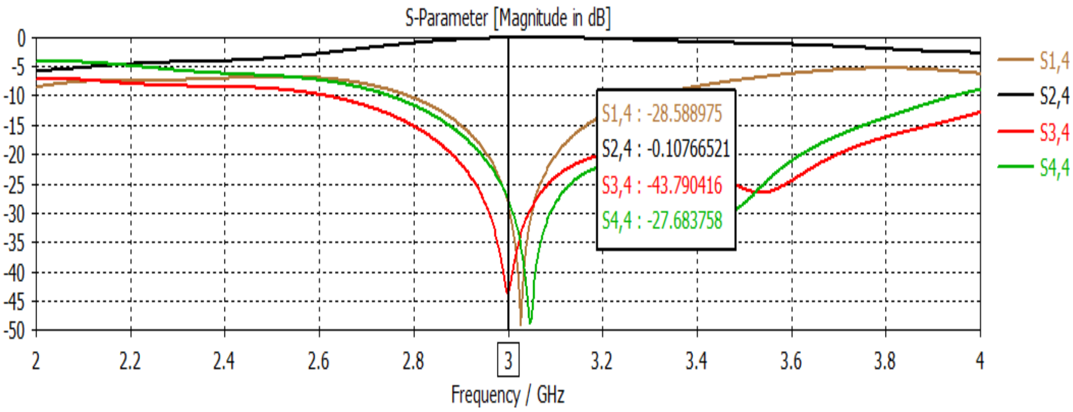

Figure 4.8: S-Parameters of a 0 dB Crossover (input port is port 4)

As shown in the previous Figures 4.7-4.8 the results demonstrate that the designed crossover works with good performance and with a high level of isolation. Therefore we can say that the purpose of this design has been acheived.

4.3 Patch Antenna

This section covers the design of the radiation element which is a microstrip patch antenna operating at 3 GHz.The design has been carried out by using feed line technique and inset feed method to achieve the matching.

The following equations have been used to obtain all parameters that will be used in our design [4].

$$W = \frac{c}{2f_r}\left(\frac{2}{\varepsilon_r + 1}\right)^{1/2} \tag{4.9}$$

$$\Delta L = 0.412\frac{(\epsilon_{reff} + 0.3)(\frac{w}{h} + 0.264)}{(\epsilon_{reff} - 0.258)(\frac{w}{h} + 0.8)}h \tag{4.10}$$

$$L_{eff} = \frac{c}{f_r\sqrt{\epsilon_{reff}}} \tag{4.11}$$

$$L = L_{eff} - 2\Delta L \tag{4.12}$$

The antenna is rectangular and operates at f_r=3 GHz, the dielectric subtrate has ε_r= 4.4 and h=1.6 mm. If we substituting these in equations (4.9-4.14), the width and the length of the rectangular patch are obtained as shown in the Table 4.5.

Table 4.5: The Dimensions of the Patch Antenna

Dimension	Calculated
Width	30.429 mm
Length	23.93mm

The layout of the rectangular patch and the simulated results (return loss and the radiation pattern) are shown in Figures 4.9-4.11.

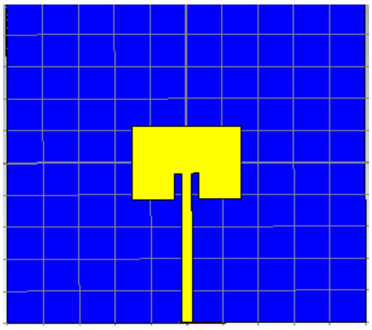

Figure 4.9: Layout of Rectangular Patch Antenna with an Insert Feed

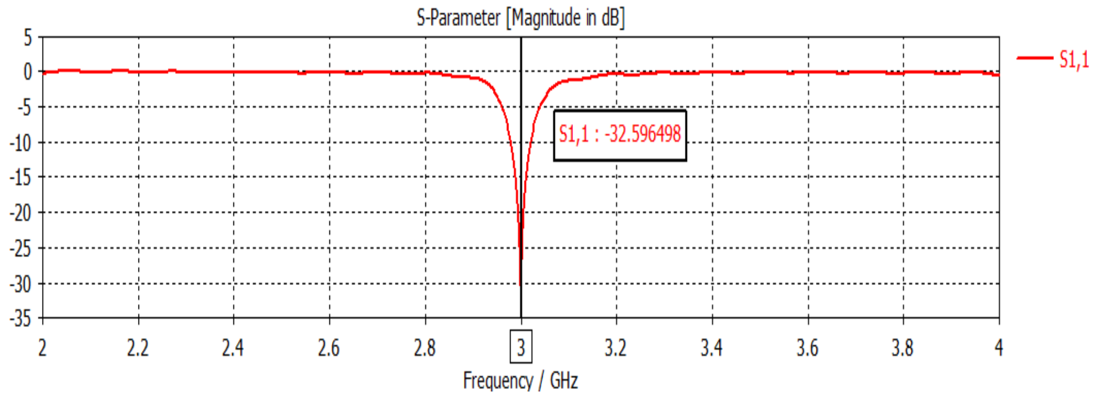

Figure 4.10: The Return Loss of the Rectangular Patch Antenna

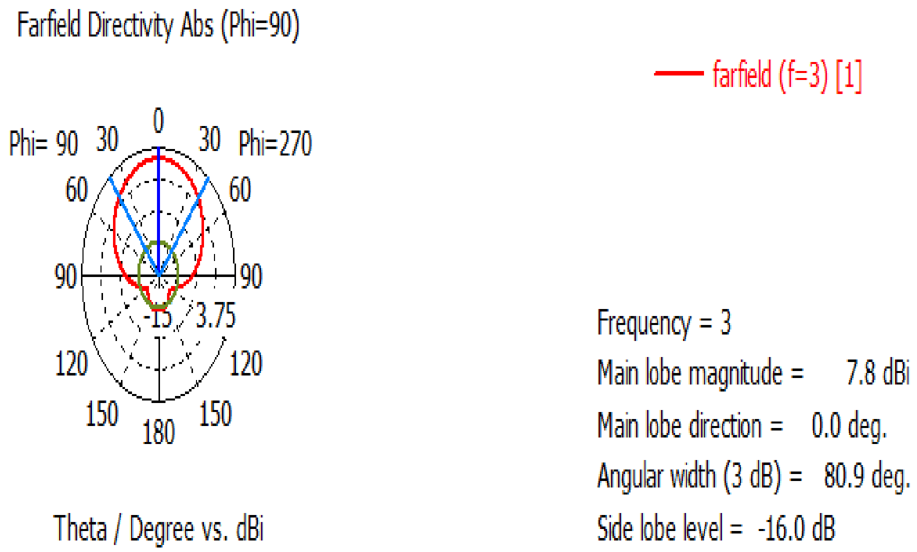

Figure 4.11: Radiation Pattern of the Rectangular Patch Antenna

As shown in the Figures 4.9-4.11 the antenna has low return loss and low level of side lobes at the design frequency.

4.4 4×4 Butler Matrix

Now we can say that all components which will be used to present the 4×4 Butler matrix are ready**.**

As for the previous components, FR-4 has been selected as a substrate having ε_r=4.4 and h=1.6mm and all components have been designed to operate at 3GHz. Our structure is shown in Figure 4.12.

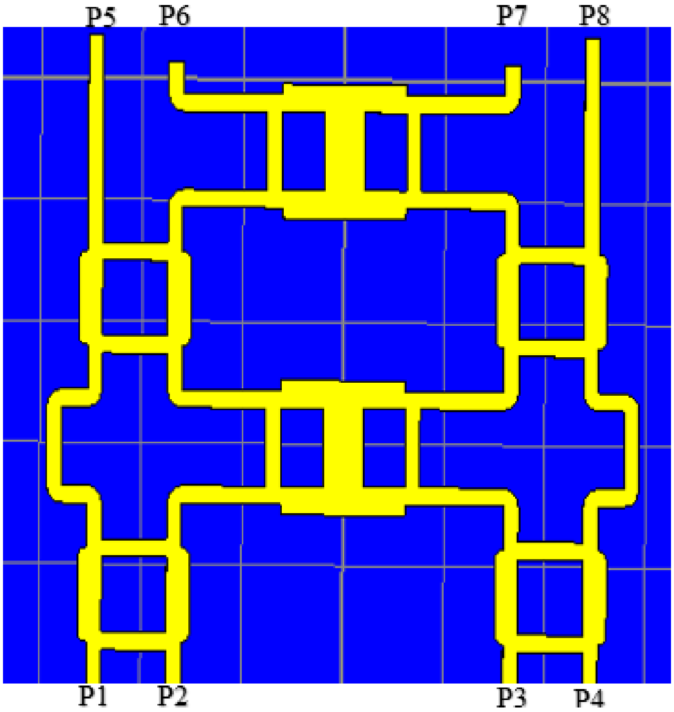

Figure 4.12: Structure of 4×4 Butler Matrix

We consider that (P1, P2, P3, P4) and (P5, P6, P7, P8) are the input and the output ports of the Butler matrix respectively as shown in the Figure 4.12.

Now each port will be excited individually and the outputs of 4×4 Butler matrix will be input for the 1×4 linear array which is shown in Figure 4.13. We have used the rectangular patch which was designed in the previous section with 0.5 λ distance elements spacing to design 1×4 linear array antenna.

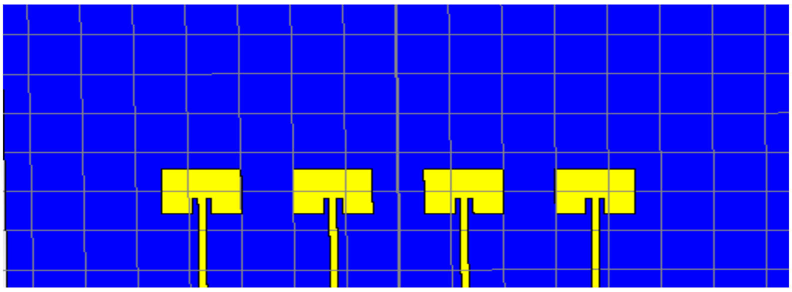
Figure 4.13: 1×4 Linear Array Antenna

When we excited P1, the scattering parameters were obtained as shown in Figure 4.14.

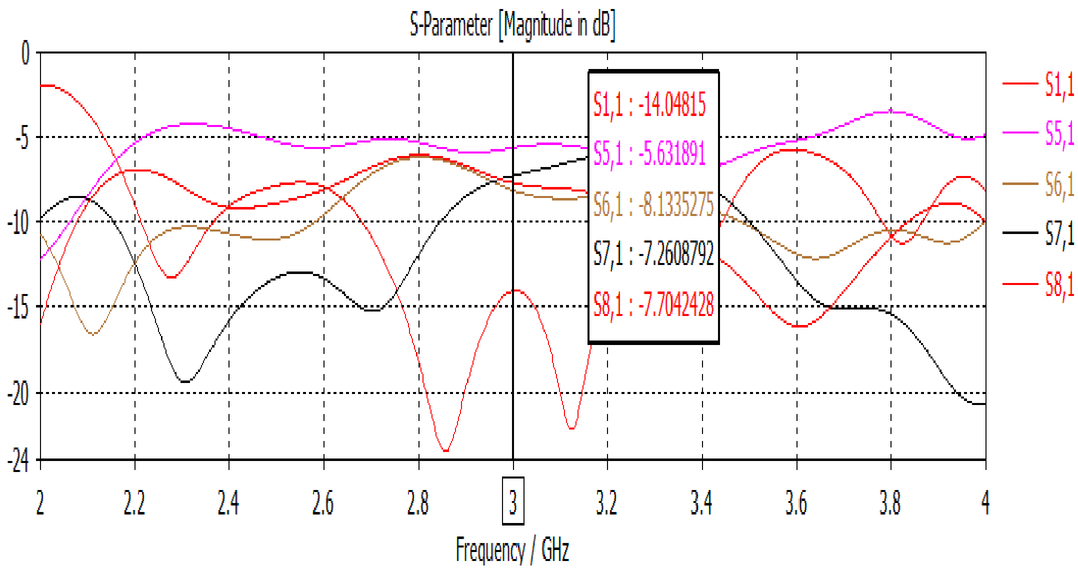

Figure 4.14: Scattering Parameters of 4×4 Butler Matrix (Excited by Port 1)

The phase differences between port 1 and the output ports of 4×4 Butler matrix are shown in figure 4.15.

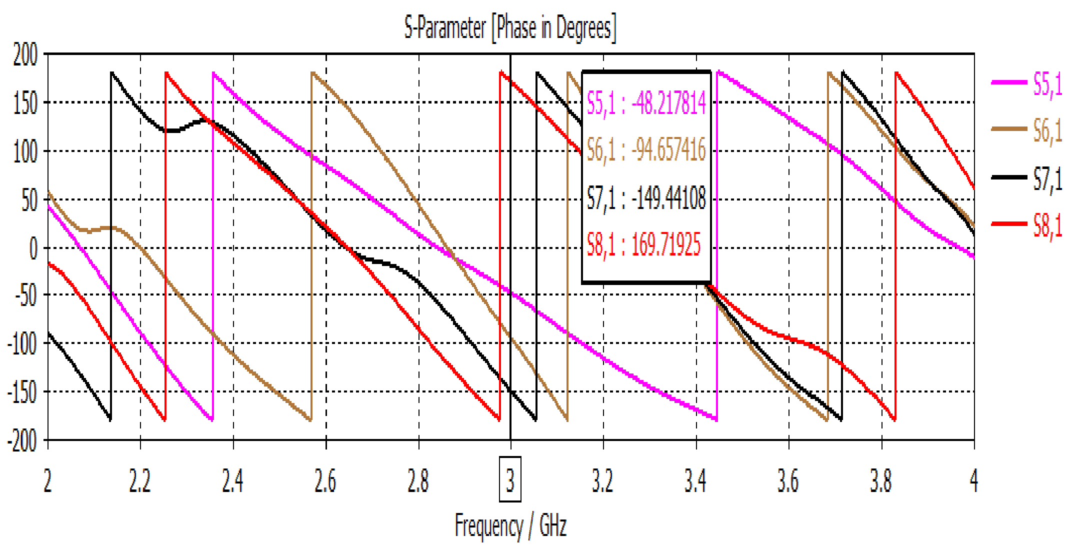

Figure 4.15: Phase Differences between port 1 and the output ports of 4×4 Butler Matrix (Excited by Port 1)

According to the Figures 4.14 and Figure 4.15, we calculate the phase differences between the outputs as shown in Table 4.6.

Table 4.6: Phase Difference between the Output Ports when Port 1 is Fed

Excitation Port	β_1 **(Port6-Port5)**	β_2 **(Port7-Port6)**	β_3 **(Port8-Port8)**	β_{AV} $(\beta_1+\beta_2+\beta_3)/3$
P1	-46.4396°	-54.7836°	-40.8398°	-47.3543°

After we have obtained the phase differences between the output ports of the Butler matrix when port 1 is fed, now we have to know the amplitude of each output port, when the Butler matrix is excited by port 1.

The sinusoidal signal has been selected as an excitation signal as shown in Figure 4.16. The amplitudes of the output signals of the simulation are shown in the Figures 4.17-4.20.

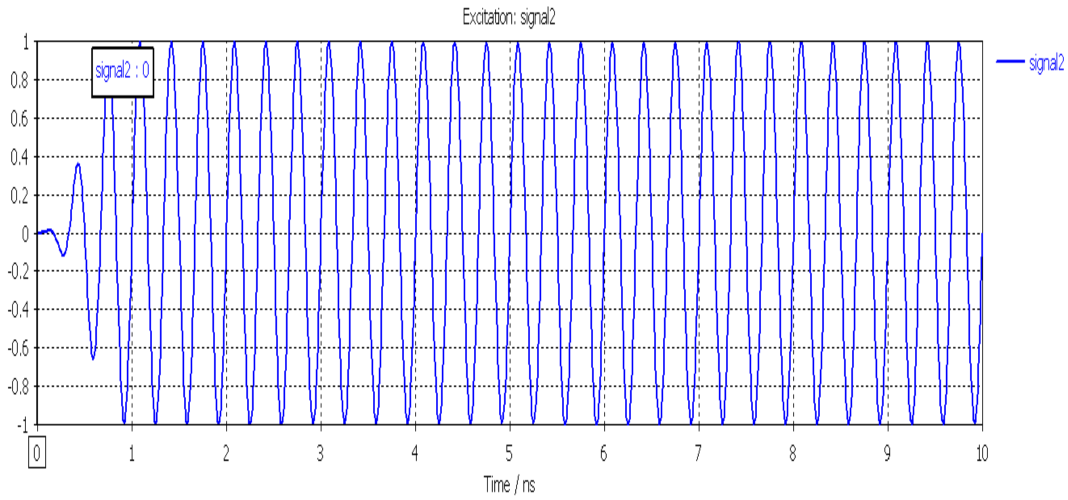

Figure 4.16: Excitation Signal (Port1)

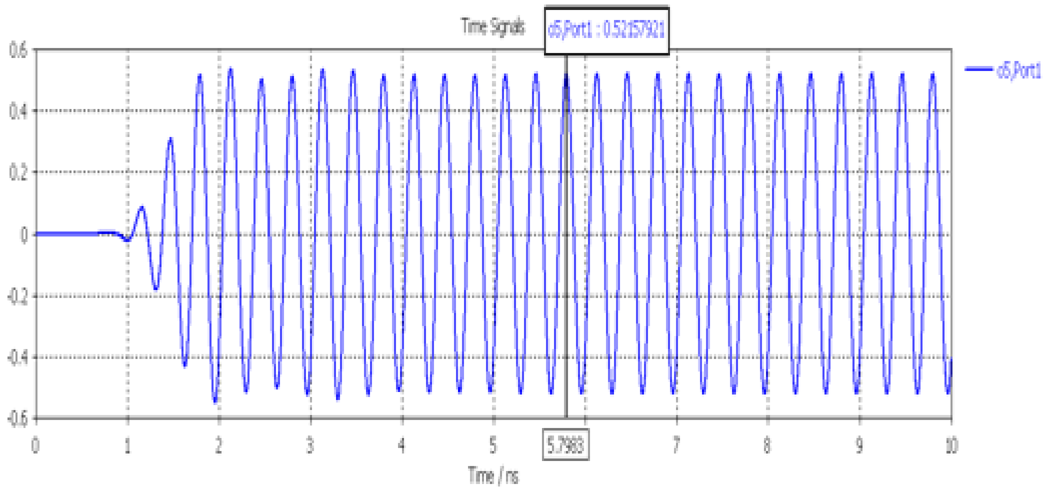

Figure 4.17: Amplitude of Port 5 (when Port 1 is Fed)

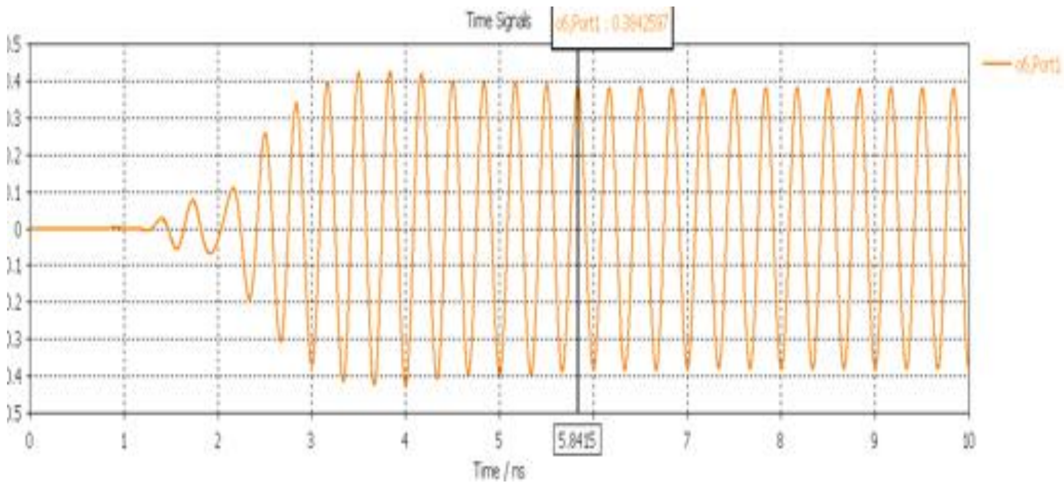

Figure 4.18: Amplitude of Port 6 (when Port1 is Fed).

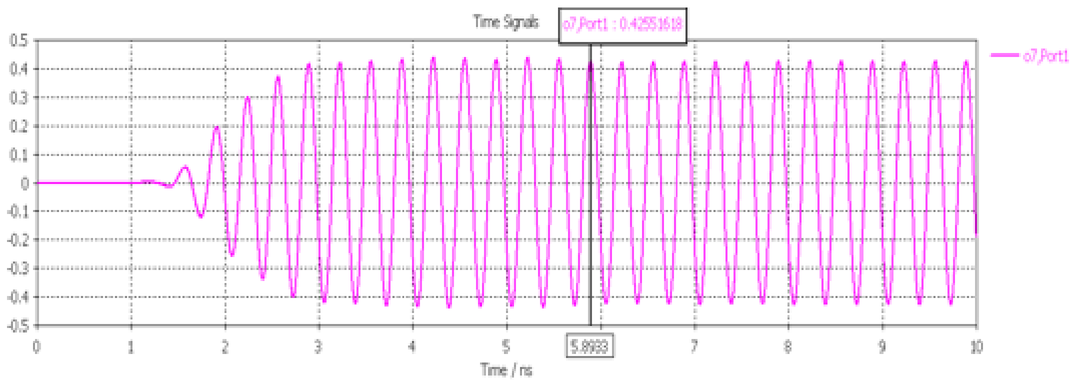

Figure 4.19: Amplitude of Port 7 (when Port 1 is Fed)

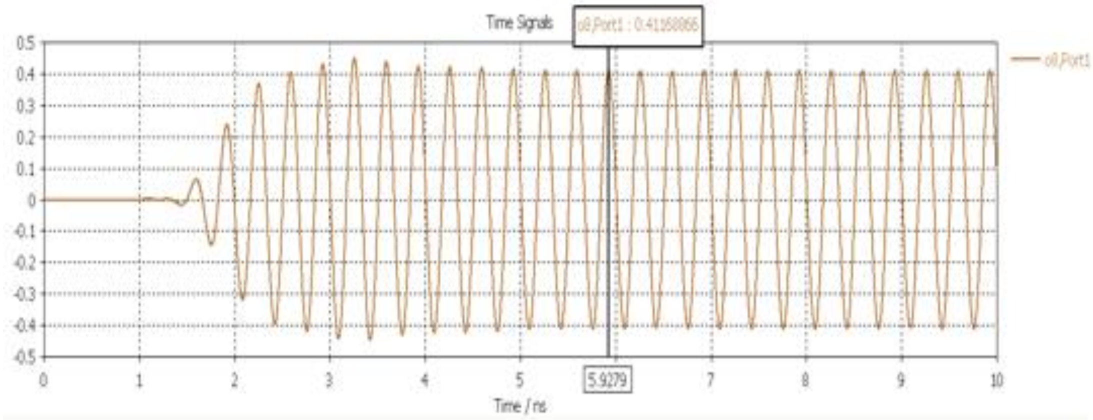

Figure 4.20: Amplitude of Port 8 (when Port 1 is Fed)

If each output of the 4×4 Butler Matrix is input in amplitude and phase for each element of the radiating array, the first beam will be achieved as shown in Figure 4.21.

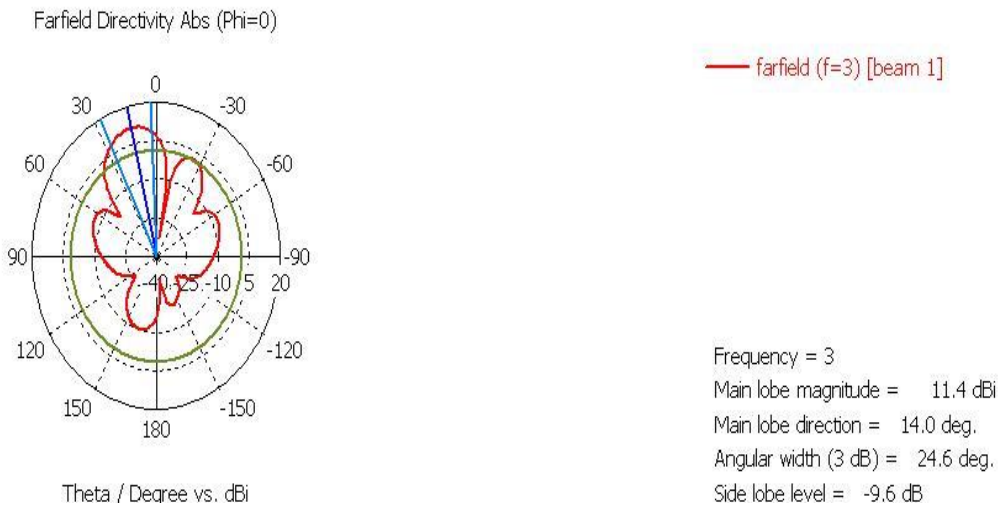

Figure 4.21: Radiation Pattern when Port 1 is Fed

When port 2 was excited, we obtained the scattering parameters shown in figure 4.22. The phase differences between port 2 and the output ports are shown in figure 4.25 and table 4.7

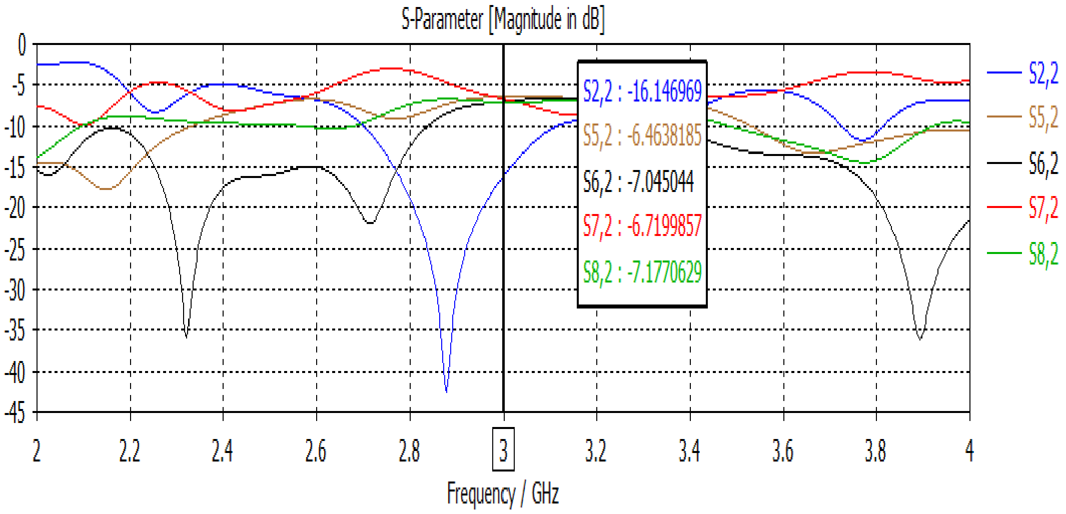

Figure 4.22: Scattering Parameters of 4×4 Butler Matrix in dB (Excited by Port 2)

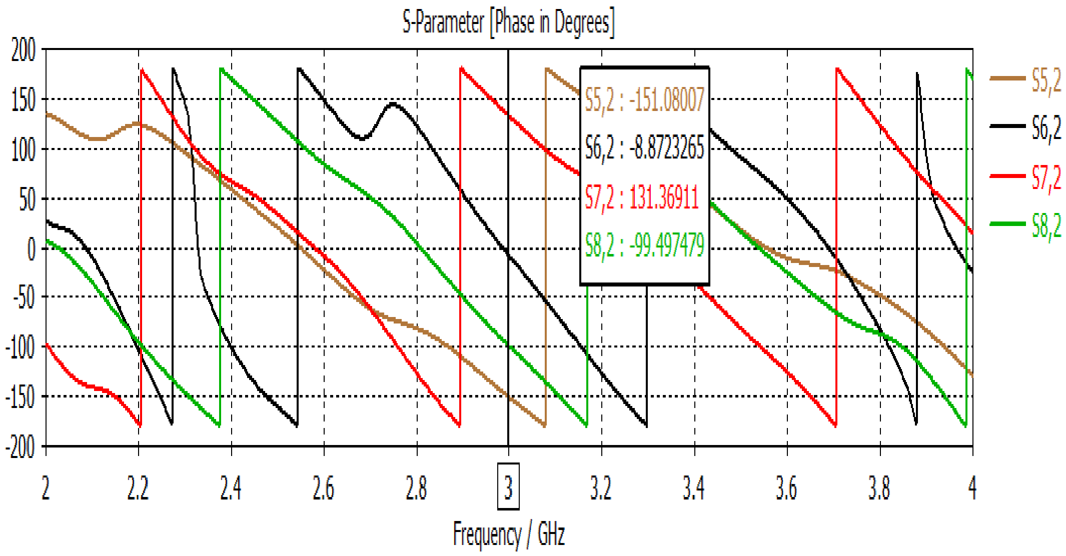

Figure 4. 23: Phase Differences between Port 2 and Output Ports of 4×4 Butler Matrix (Excited by Port 2)

Table 4.7: Phase Differences between the Output Ports when Port 2 is Fed

Excitation Port	β_1 **(Port6-Port5)**	β_2 **(Port7-Port6)**	β_3 **(Port8-Port8)**	β_{AV} $(\beta_1+\beta_2+\beta_3)/3$
P2	142.2077°	140.2414°	129.1335°	137.1942°

The excitation signal that is shown in Figure 4.16 has also been selected to apply on port 2, then the output signals will be as shown in Figures 4.24 - 4.27.

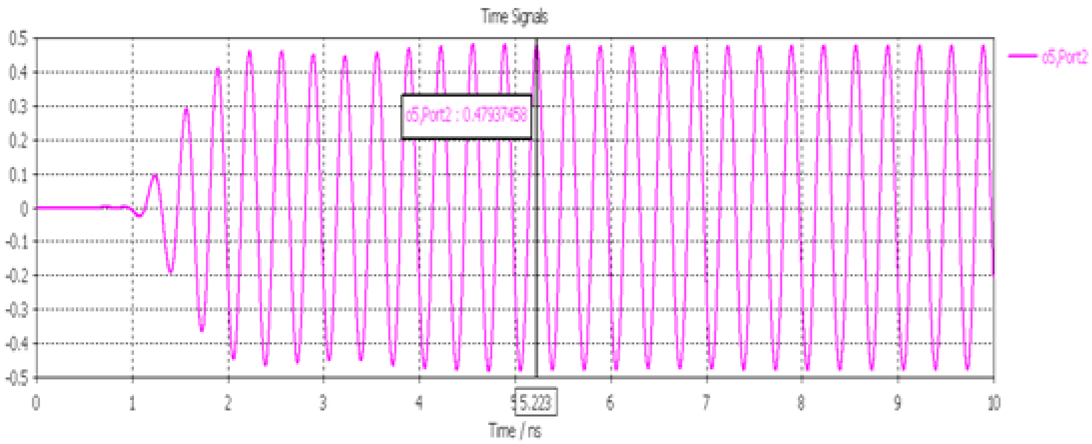

Figure 4.24: Amplitude of Port 5 (when Port 2 is Fed)

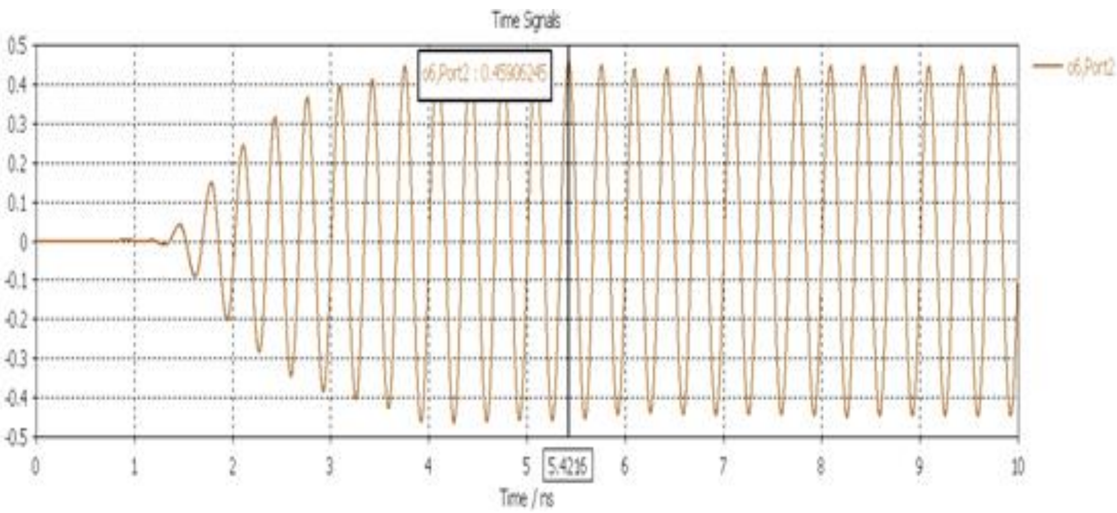

Figure 4.25: Amplitude of Port 6 (when Port 2 is Fed)

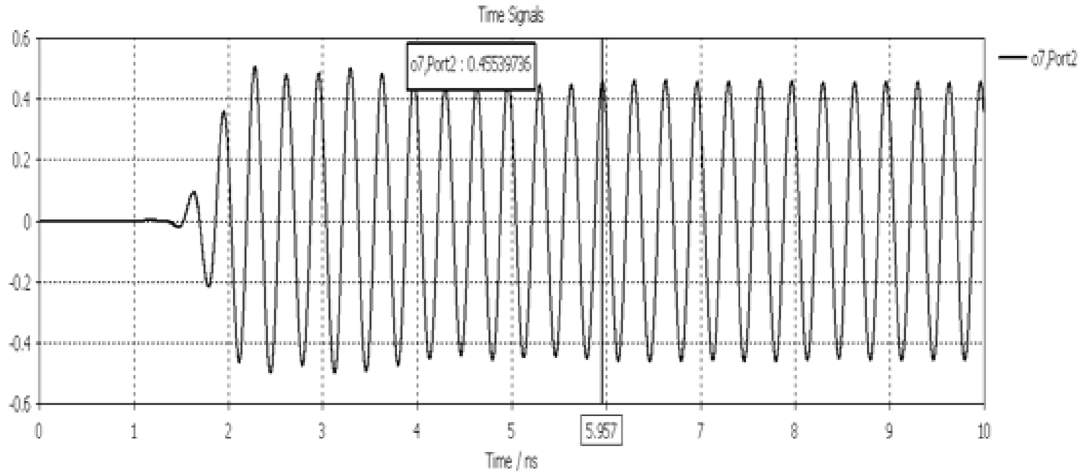

Figure 4.26: Amplitude of Port 7 (when Port 2 is Fed)

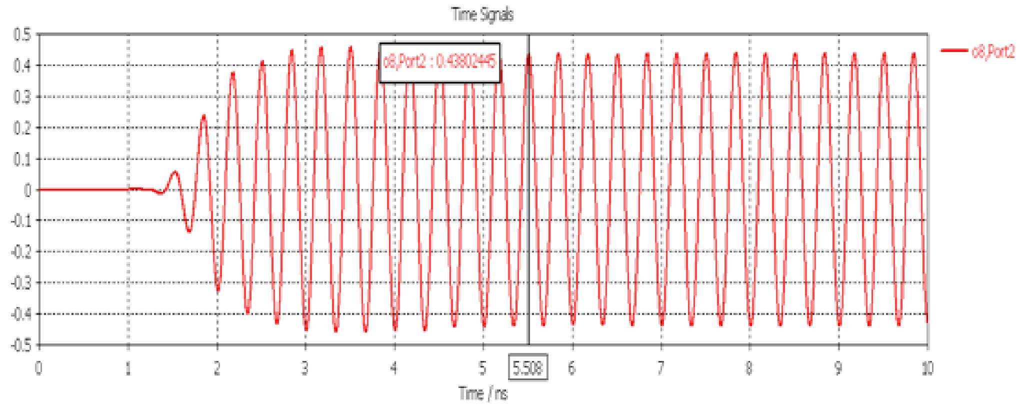

Figure 4.27: Amplitude of Port 8 (when Port 2 is Fed)

When we apply the outputs of 4×4 Butler Matrix (as amplitude and phase) to the inputs of array antenna Figure 4.13, the second beam will be as shown in Figure 4.28

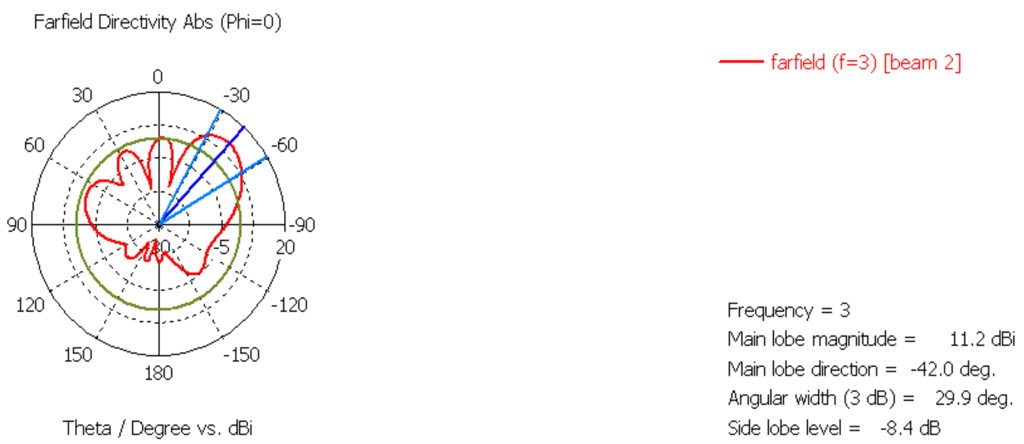

Figure 4.28: Radiation Pattern when Port 2 is Fed

Now we are going to observe the simulation results, the phase differences and the radiation pattern of the antenna when 4×4 Butler matrix has been fed by port 3. Figure 4.29, and the phase differences between port 3 and the output ports are shown in Figure 4.30.

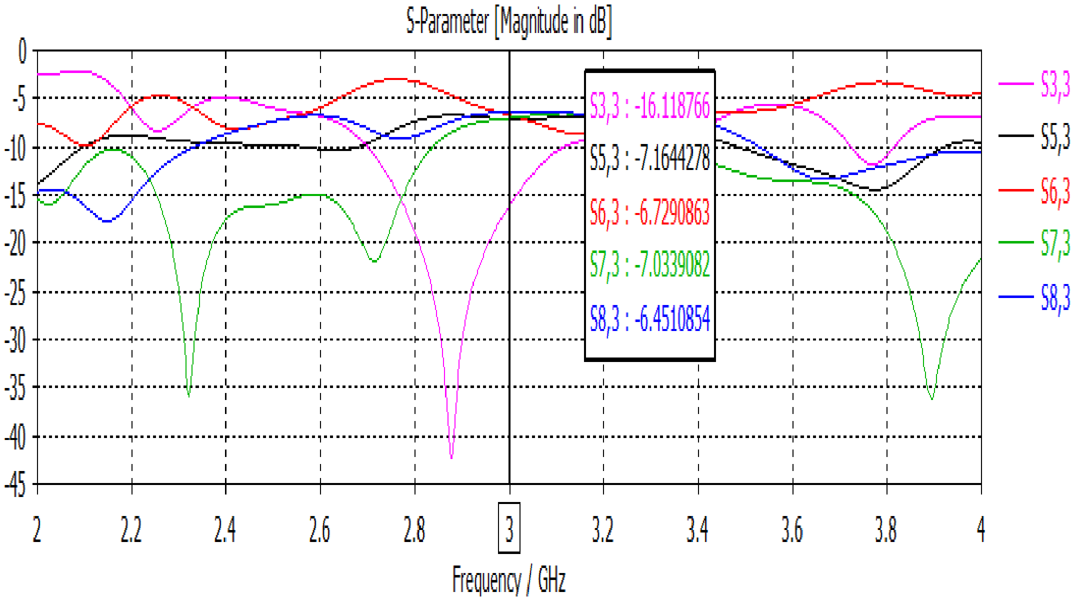

Figure 4.29: Scattering Parameters of 4×4 Butler Matrix in dB (Excited by Port 3)

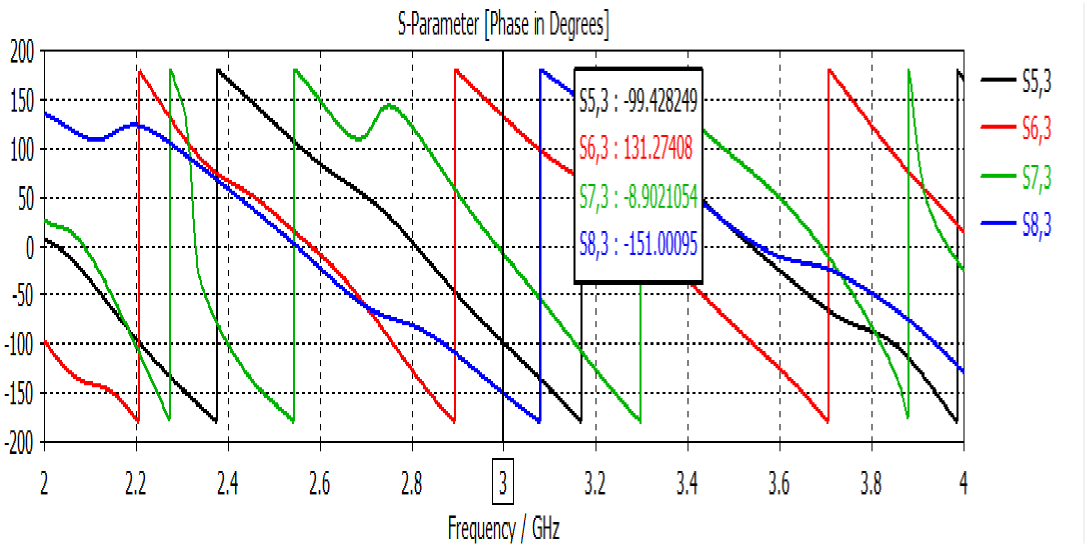

Figure 4.30: Phase Differences between Port 3 and Output Ports of 4×4 Butler Matrix (Excited by Port 3)

The phase differences of the output ports when port 3 is fed are listed in table 4.8, and the radiation pattern is shown in figure 3.31.

Table 4.8: Phase Differences between the Output Ports when port 3 is fed

Excitation Port	$\boldsymbol{\beta_1}$ **(Port6-Port5)**	$\boldsymbol{\beta_2}$ **(Port7-Port6)**	$\boldsymbol{\beta_3}$ **(Port8-Port8)**	$\boldsymbol{\beta_{AV}}$ $\boldsymbol{(\beta_1 + \beta_2 + \beta_3)/3}$
P3	-129.2975°	-140.1761°	-142.0988°	-137.1908°

The amplitudes of the output signals are approximately equal to the amplitude of the output signal when the Butler matrix was fed by port 2.

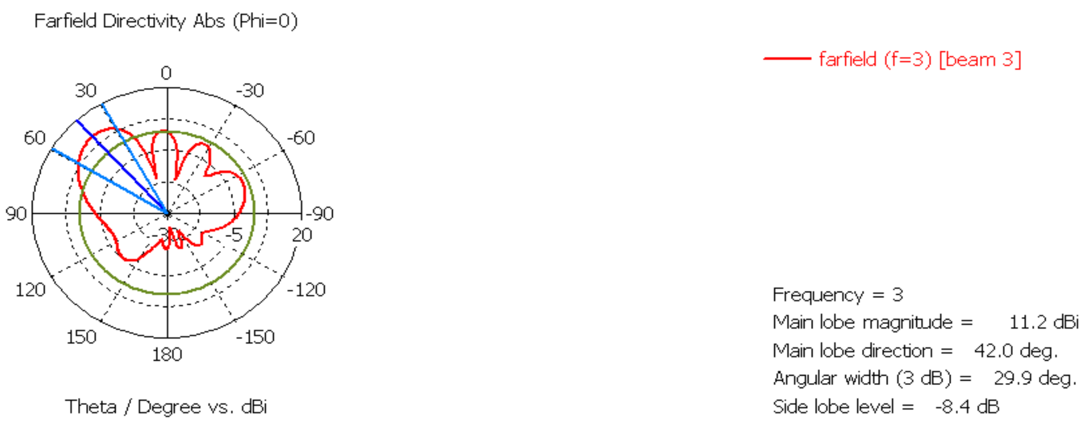

Figure 4.31: Radiation Pattern When Port 3 is Fed

Similar to the other ports when the Butler matrix is fed by port 4, the scattering parameters and the phase differences between port 4 and the output ports and the radiation pattern are shown in Figure 4.32, Figure4.33, and Figure 4.34 respectively.

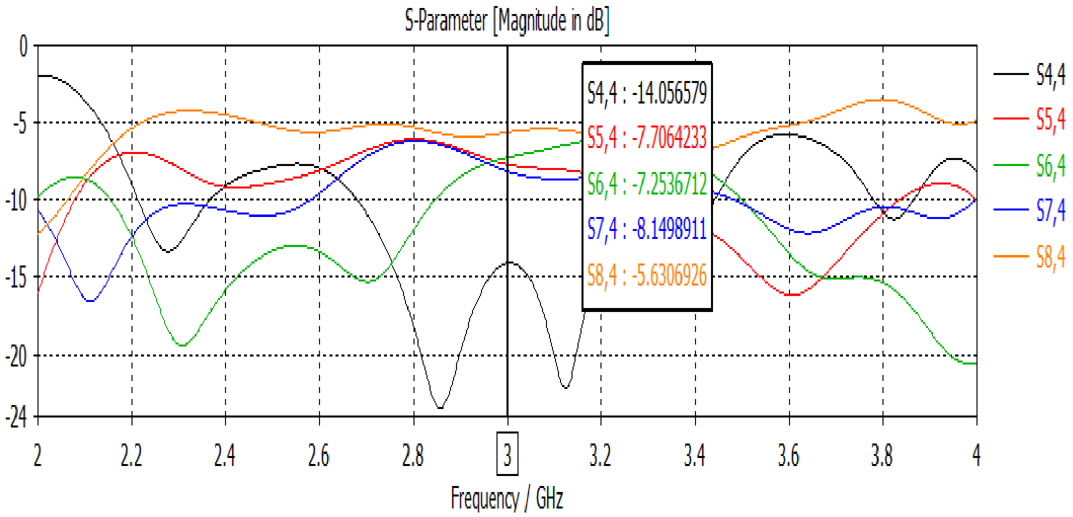

Figure 4.32: Scattering Parameters of 4×4 Butler Matrix in dB (Excited by Port 4)

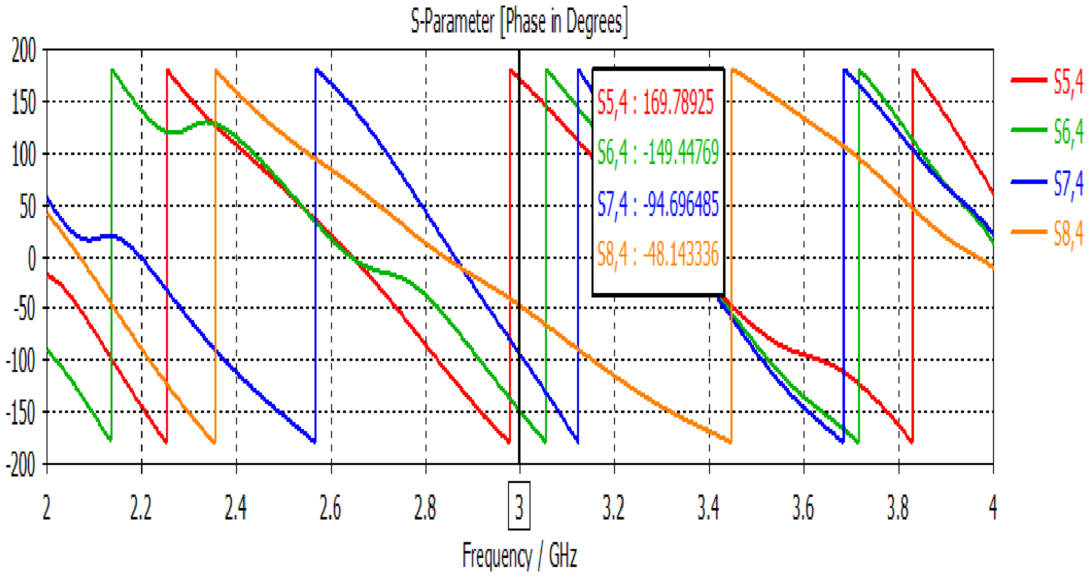

Figure 4.33: Phase Differences between port 1 and the Output Ports of 4×4 Butler Matrix (Excited by Port 4)

The phase differences between the output ports when port 4 is fed are listed in table 4.9.

Table 4.9: Phase Differences between the Output Ports when port 4 is fed

Excitation Port	β_1 (Port6-Port5)	β_2 (Port7-Port6)	β_3 (Port8-Port8)	β_{AV} $(\beta_1 + \beta_2 + \beta_3)/3$
P4	40.7932°	54.7512°	46.5531	47.3658°

The amplitudes of the output signals are approximately equal to the amplitude of the output signal when the Butler matrix was fed by port 1.

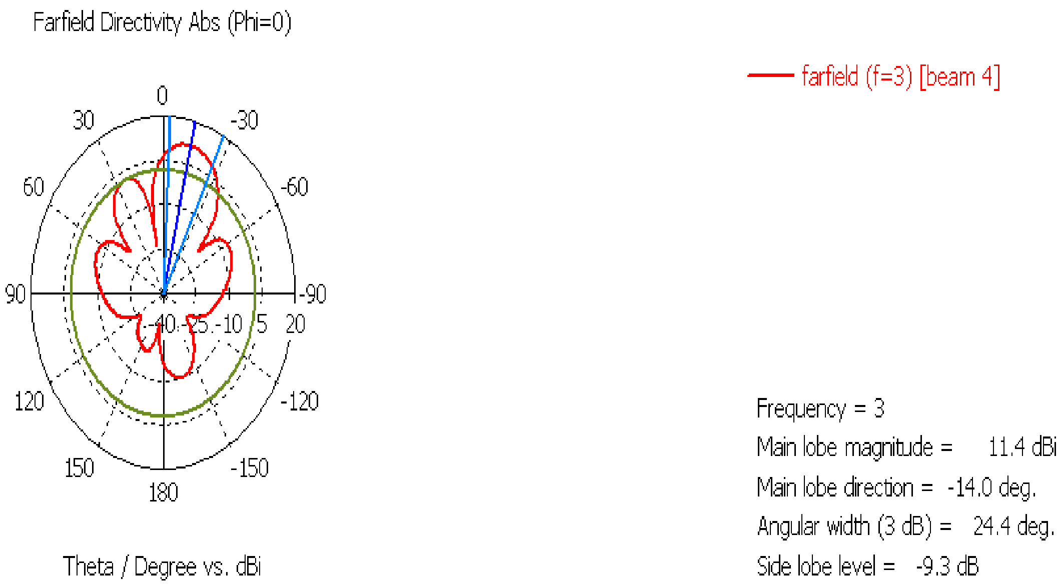

Figure 4.34: Radiation Pattern When Port 4 is Fed

Now we can say the design of 4×4 Butler Matrix to operate at 3GHz frequency has been achieved. We can see the four beams together in Cartesian plot as shown in Figure 4.35.

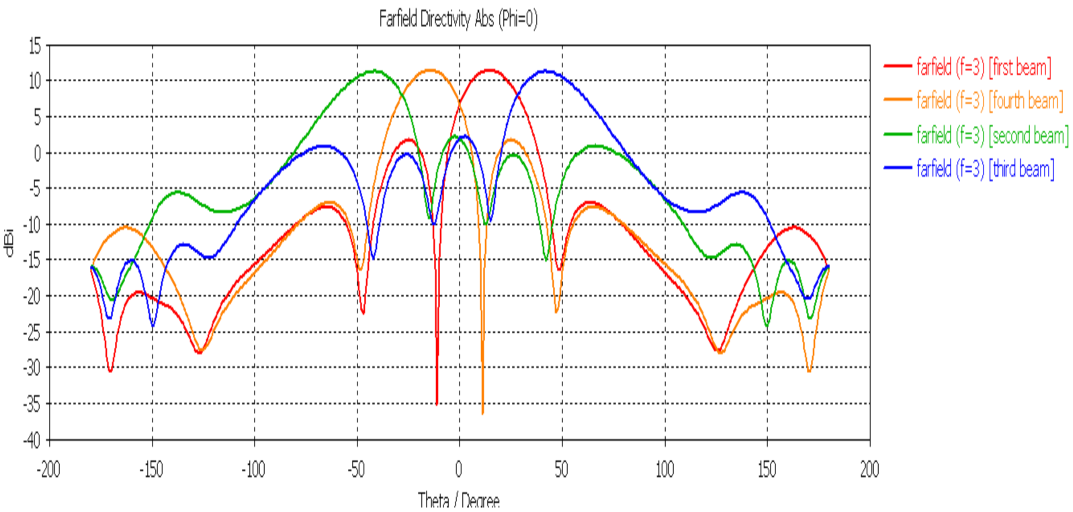

Figure 4.35: Combination of Four Beams of 4×4 Butler Matrix

4.5 Generating New Beam for 4×4 Butler Matrix

The Butler matrix was modified to obtain a beam to in the 0˚direction in addition to other four beams that we have obtained. Before presenting the proposed design, understanding the use of directional couplers as a power dividers is essintial.

The dirctional coupler works as a power divider but in our case we have done a modification to achieve 0˚phase shift between the oututs. Suppose that port 1 is the input port, adding an extra length of $\lambda_g/4$ for the quadrature coupler to port 2 changes the phase diffrence. Port 4 remains unused and is termatened with a 50 Ω matching load as shown in Figure 4.36.

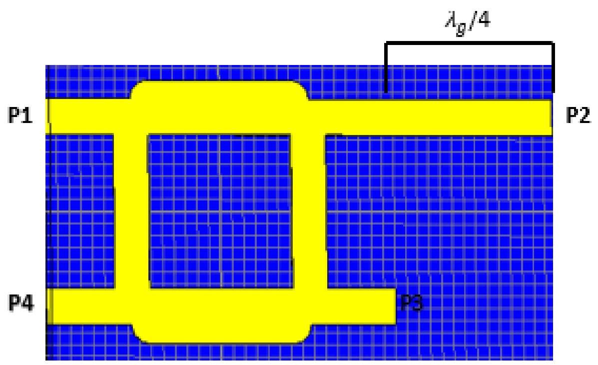

Figure 4.36: Directional Coupler with a 0˚Phase Shift

The calculated length of $\lambda_g/4$ is 13.6 mm, this value has been optimised to 13.78 mm for better performance. The simulated S-parameters and phase diference between the output ports are shown in figure 4.37 and figure 4.38 respectively.

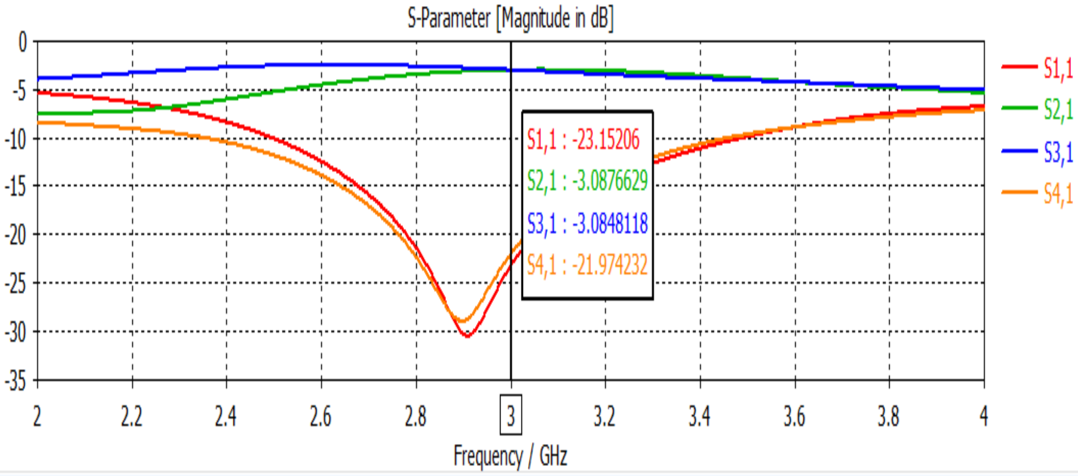

Figure 4.37: Simulation Results of Directional Coupler with a 0˚Phase Shift (in dB)

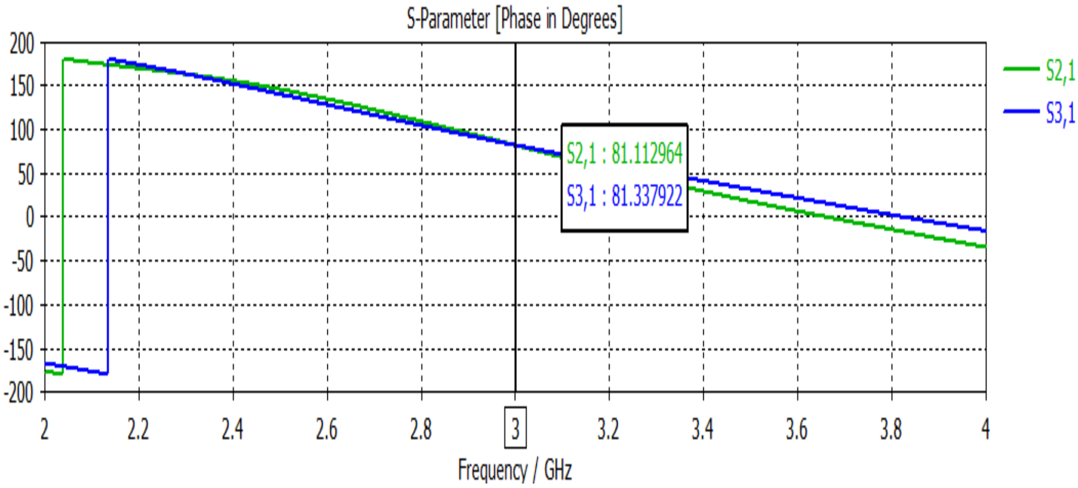

Figure 4.38: The Phase Diffirence between the Output Ports of a Directional Coupler with a 0˚Phase ShifT

According to Figure 4.37 and Figure 4.38 the power will be divided equally between the output ports with approximately 0˚phase shift (0.225˚difference).

The first step that we proposed to modify the Butler matrix is the duplication of the input ports using the modified directional coupler as shown in Figure 4.39. The duplication is done in order to maintain the original beams.

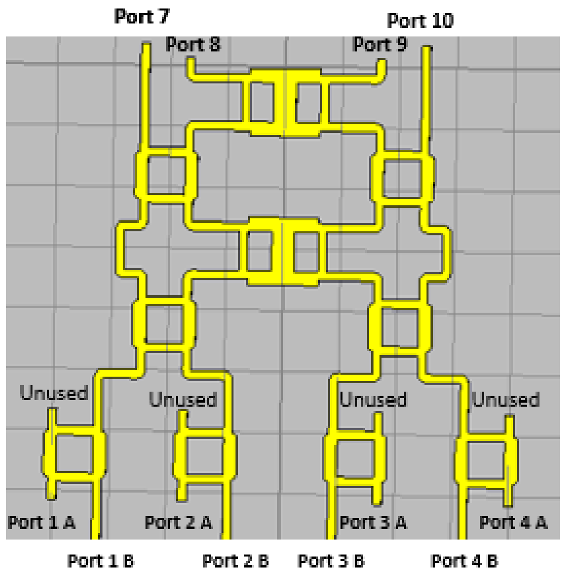

Figure 4.40: Douplicating of 4×4 Butler Matrix Ports Using Directional Coupler

As shown in the Figure 4.40, the input ports have been duplicated using a directional coupler. We have two copies A and B of each port. Ports 1A, 2A, 3A and 4A represent the main four beams, while ports opposite to them are terminated by 50 Ω matching loads. Figures 4.41-4.44 show the phase differences between the main beams ports and the output ports for the modified structure. It can be seen that the phase difference sets in the modified structure where maintained.

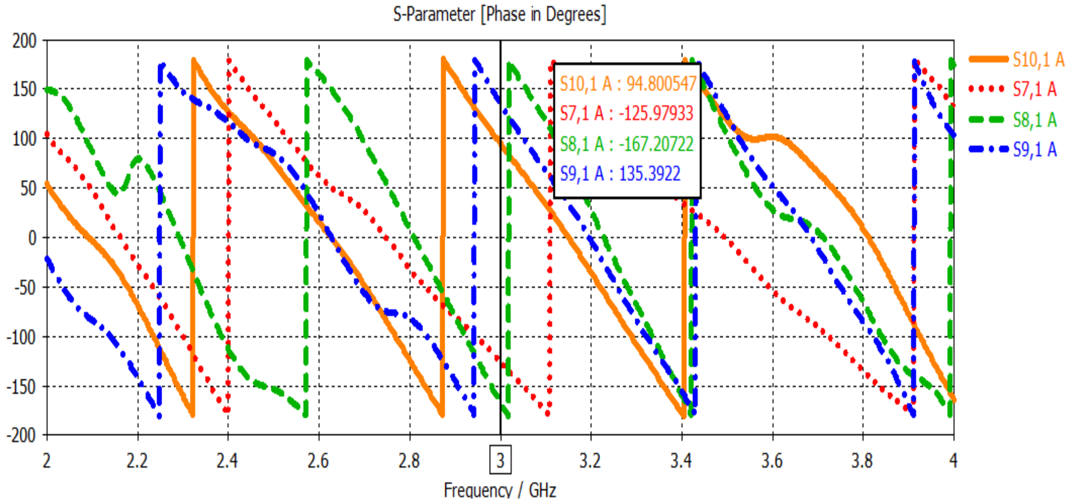

Figure 4.41: The Phase Differences between Port 1A and the Output Ports of the Modified Butler Matrix

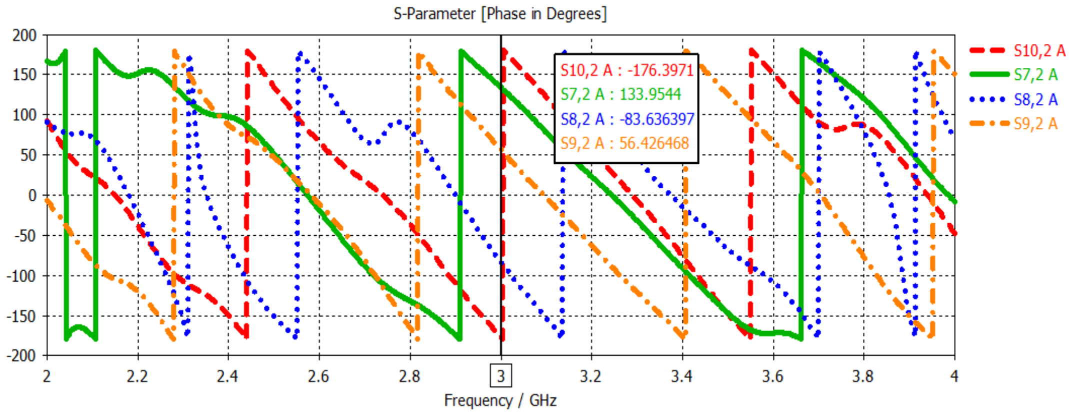

Figure 4.42: The Phase Differences between Port 2A and the Output Ports of the Modified Butler Matrix

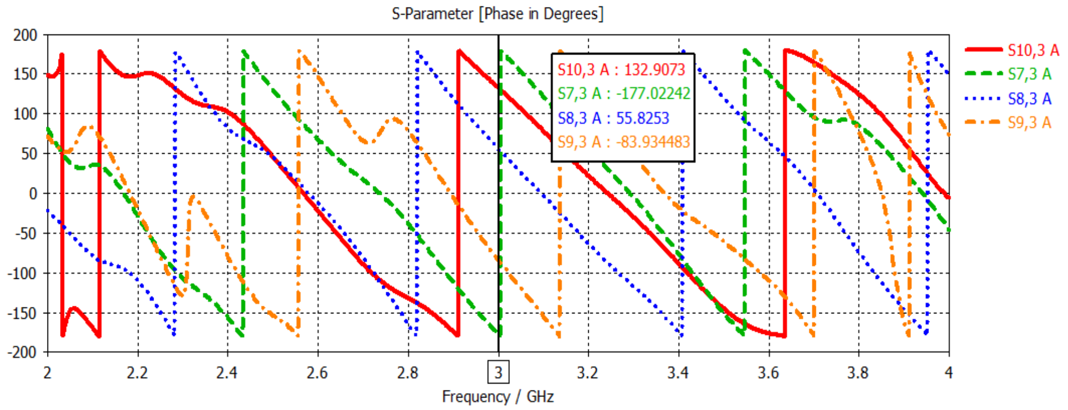

Figure 4.43: The Phase Differences between Port 3A and the Output Ports of the Modified Butler Matrix

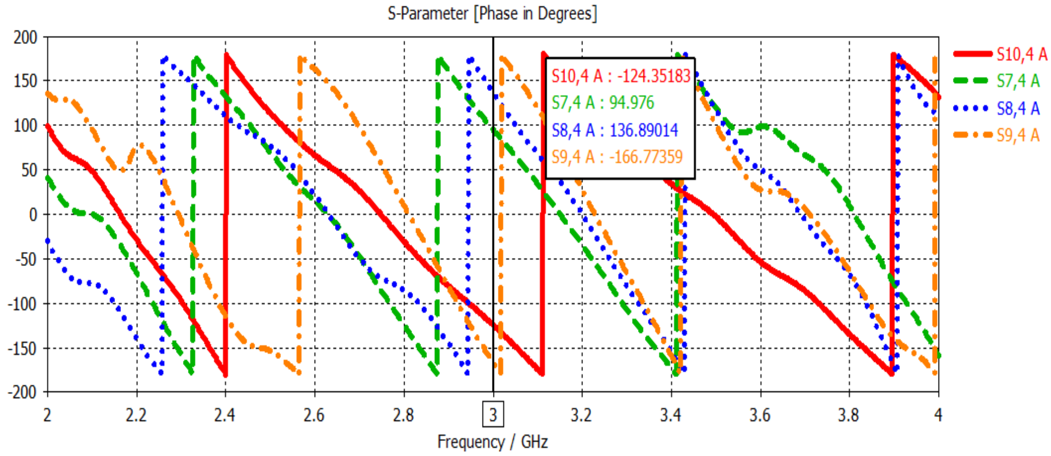

Figure 4.44: The Phase Differences between Port 4A and the Output Ports of the Modified Butler Matrix

These phase differences have been used to obtain the main four beam that are shown in Figure 4.45.

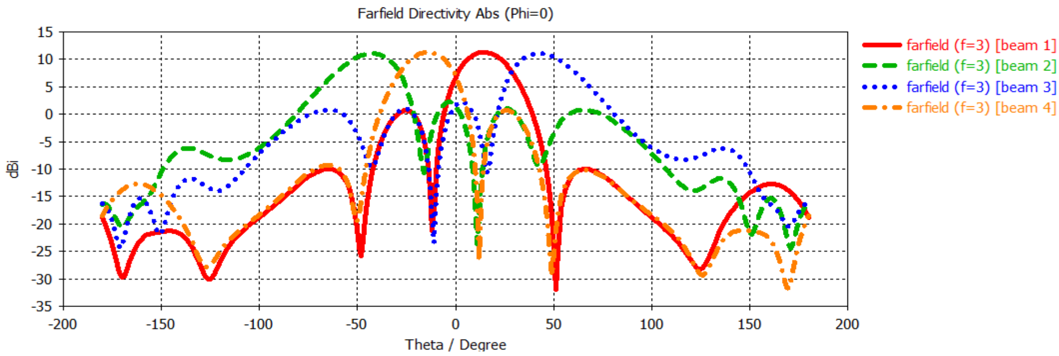

Figure 4.45: The Combination of the Four Main Beams of Modified Butler Matrix

The modified directional coupler has been used to combine port 1B and port 2B in one port which is port 5A, and combine port 3B and port 4B in one port which is port 5B, as shown in Figure 4.46. We have to take into account that the ports which are in the same side of ports 5A and 5B are terminated by 50 Ω matching loads, because they are not used.

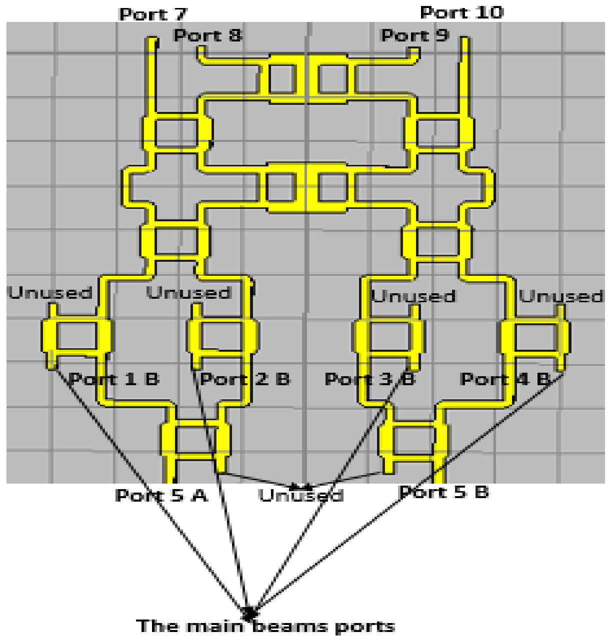

Figure 4.46: combining port 1B and port 2B in port 5A and combining Port 3B and Port 4B in port 5B

The final step of our proposed design has been done using the modified directional coupler, which combines port 5A and port 5B in port 5, as shown in Figure 4.47.

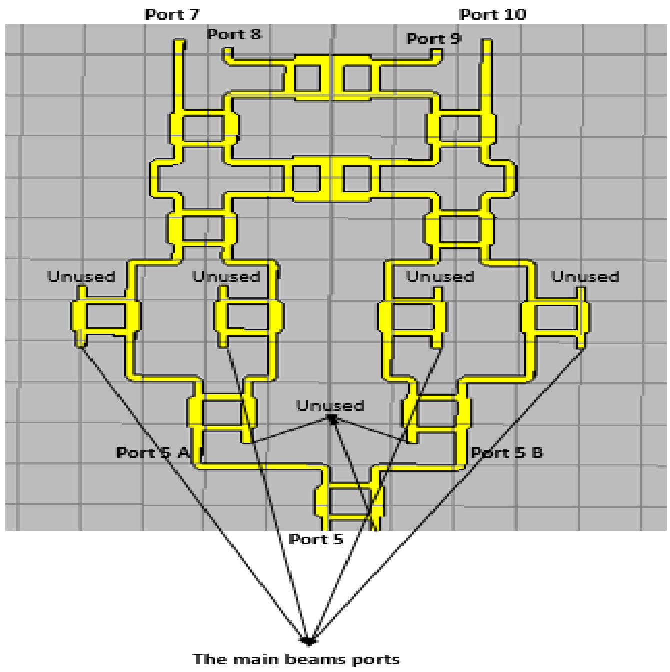

Figure 4.47: Modification of the Butler Matrix to Generate Fifth Beam

The fifth beam has been generated by the excitation of port 5, the phase differences between port 5 and the output ports and the fifth beam which is at 0° are shown in figure 4.48 and figure 4.49.

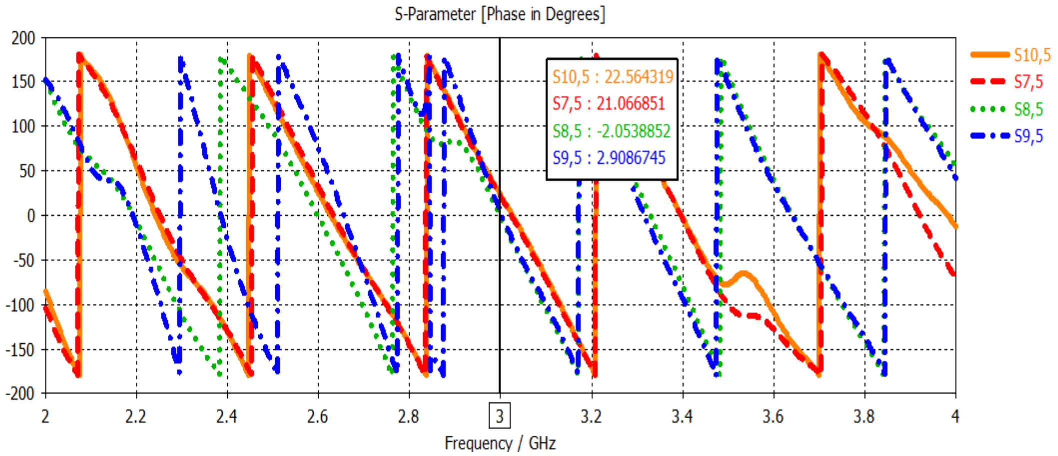

Figure 4.48: The Phase Differences between Port 5 and the Output Ports of the Modified Butler Matrix

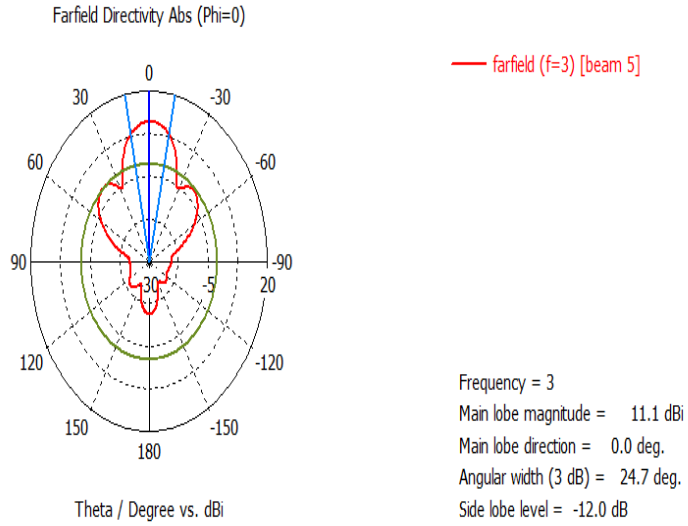

Figure 4.49: Radiation Pattern of the Modified Butler Matrix when Port 5 is Fed

The fifth beam has been added to the main four beams as shown in Figure 4.50.

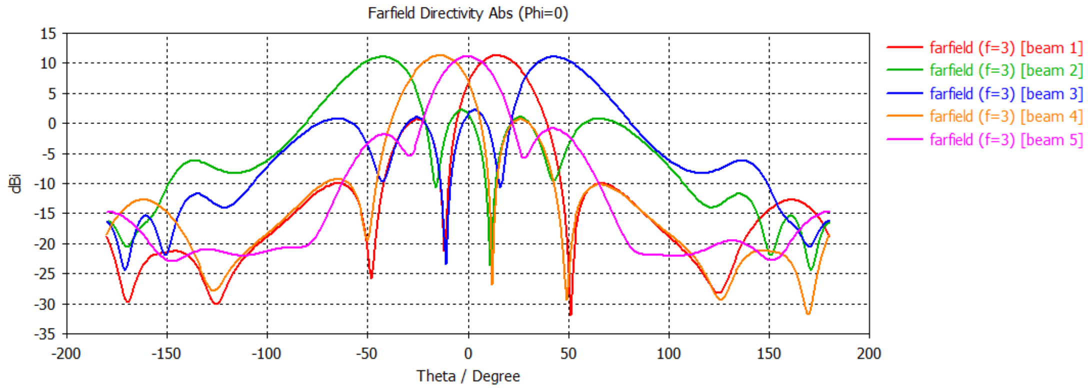

Figure 4.50: Combination of the Five Beams of the Modified Butler Matrix

Chapter 5

CONCLUSION

In this thesis one of the beamforming networks (Butler matrix) has been presented. The study carried out by using the CST MICROWAVE STUDIO SUIT.

According to the simulation results that have been achieved in this work, a switched-beamforming network at 3 GHz has been designed to obtain four orthogonal beams at -14°,-42°, 42° and 14°. The beams have 24.6°, 29.9°, 29.9°and 24.4° HPBW and gain of 11.4 dB, 11.2 dB, 11.2dB, and 11.4dB with -9.6dB, -8.4dB, -8.4 dB, and -9.3 dB SSL respectively. The size of 4×4 butler matrix is (104 mm×100 mm).

A fifth beam has been generated in the broadside direction of the antenna by a slight modification on the Butler matrix. The new beam has 24.7 HPBW and a gain of 11.1dB with -12 SSL. The size of the modified structure is (240 mm×164 mm).

The original beams have been maintained in the same directions. The proposed design increases the coverage area.

REFERENCES

[1] Gotsis, K. A., Siakavara, K., & Sahalos, J. N. (2009). On the direction of arrival (DoA) estimation for a switched-beam antenna system using neural networks. *IEEE Transactions on Antennas and Propagation*, *57*(5), 1399-1411.

[2] Alexiou, A., &Haardt, M. (2004). Smart antenna technologies for future wireless systems: trends and challenges. *IEEE Communications Magazine*, *42*(9), 90-97.

[3] Ren, h. (2013). *Design and application of phased array system* (m.sc). University of North Texas.

[4] Balanis, C. A. (2016). *Antenna theory: analysis and design*. John Wiley & Sons.

[5] Balanis, C. A., &Ioannides, P. I. (2007). Introduction to smart antennas. *Synthesis Lectures on Antennas*, *2*(1), 1-175.

[6] Fakoukakis, F. E., &Kyriacou, F. G. (2011, September). On the design of a Butler matrix-based beamformer introducing low sidelobe level and enhanced beam-pointing accuracy. In *Antennas and Propagation in Wireless Communications (APWC), 2011 IEEE-APS Topical Conference on* (pp. 1265-1268). IEEE.

[7] Ibrahim, S. Z., & Rahim, M. K. A. (2007, December). Switched beam antenna using omnidirectional antenna array. In *Applied Electromagnetics, 2007. APACE 2007. Asia-Pacific Conference on* (pp. 1-4). IEEE.

[8] Kadir, M. A., Rose, M. C., Shah, M. M., Misman, D., Suaidi, M. K., & Aziz, M. A. (2007, December). 4x4 Butler Matrix design by using circular bend. In *Applied Electromagnetics, 2007. APACE 2007. Asia-Pacific Conference on* (pp. 1-5). IEEE.

[9] Ajiboye, S., & Wang, Y. (2013, September). Investigation on the interfering effect of feeding network on the performance of a beamforming antenna array. In *AFRICON, 2013* (pp. 1-4). IEEE.

[10] Kaifas, T. N., & Sahalos, J. N. (2006). On the design of a single-layer wideband Butler matrix for switched-beam UMTS system applications [Wireless Corner]. *IEEE Antennas and Propagation Magazine*, *48*(6), 193-204.

[11] Sahu, B. Design and Implementation of 4x4 Butler Matrix.

[12] Siachalou, E., Vafiadis, E., Goudos, S. S., Samaras, T., Koukourlis, C. S., &Panas, S. (2004). On the design of switched-beam wideband base stations. *IEEE Antennas and Propagation Magazine*, *46*(1), 158-167.

[13] Li, W. R., Chu, C. Y., Lin, K. H., & Chang, S. F. (2004). Switched-beam antenna based on modified Butler matrix with low sidelobe level. *Electronics Letters*, *40*(5), 290-292.

[14] Denidni, T. A., &Libar, T. E. (2003, September). Wide band four-port butler matrix for switched multibeam antenna arrays. In *Personal, Indoor and Mobile*

Radio Communications, 2003. PIMRC 2003. 14th IEEE Proceedings on (Vol. 3, pp. 2461-2464). IEEE.

[15] Moubadir, M., Bayjja, M., Touhami, N. A., Aghoutane, M., &Tazon, A. (2015, October). Design and implementation of a technology planar 8× 8 Butler matrix with square truncated Edge-Fed array antenna for WLAN networks application. In *Wireless Networks and Mobile Communications (WINCOM), 2015 International Conference on* (pp. 1-5). IEEE.

[16] Fakoukakis, F. E., Kyriacou, G. A., &Sahalos, J. N. (2012, March). On the design of Butler-like type matrices for low SLL multibeam antennas. In *Antennas and Propagation (EUCAP), 2012 6th European Conference on* (pp. 2604-2608). IEEE.

[17] Wincza, K., Gruszczynski, S., &Sachse, K. (2008). Conformal four-beam antenna arrays with reduced sidelobes. *Electronics Letters*, *44*(3), 17.

[18] James, J. R., Hall, P. S., & Wood, C. (1985). *Microstrip antenna: theory and design* (No. 12). Iet.

[19] Pozar, D. M. (1992). Microstrip antennas. *Proceedings of the IEEE*, *80*(1), 79-91.

[20] Uzunoglu, N., Alexopoulos, N., & Fikioris, J. (1979). Radiation properties of microstrip dipoles. *IEEE Transactions on Antennas and Propagation*, *27*(6), 853-858.

[21] Singh, G., & Singh, J. (2012). Comparative Analysis of Microstrip Patch Antenna With Different Feeding Techniques. In *International Conference on Recent Advances and Future Trends in Information Technology, iRAFIT*.

[22] Bist, S., Saini, S., Prakash, V., &Nautiyal, B. (2014). Study The Various Feeding Techniques of Microstrip Antenna Using Design and Simulation Using CST Microwave Studio. *International Journal of Emerging Technology and Advanced Engineering*, *4*(9).

[23] Ali, M. T., Muhamud, S., Rahman, N. A., &Ya'acob, N. (2011, June). A microstrip patch antenna with aperture coupler technique at 5.8 GHz. In *System Engineering and Technology (ICSET), 2011 IEEE International Conference on* (pp. 121-124). IEEE.

[24] Garg, R. (2001). *Microstrip antenna design handbook*. Artech house.

[25] Sastry, I. R., & Sankar, K. J. (2014). Proximity Coupled Rectangular Microstrip Antenna with X-slot for WLAN Application. *Global Journal of Research and Engineering-GJRE-F*, *14*(1).

[26] Carver, K., & Mink, J. (1981). Microstrip antenna technology. *IEEE transactions on antennas and propagation*, *29*(1), 2-24.

[27] Hong, J. S. G., & Lancaster, M. J. (2004). *Microstrip filters for RF/microwave applications* (Vol. 167). John Wiley & Sons.

[28] Nakar, P. S. (2017). Design of a compact microstrip patch antenna for use in wireless/cellular devices.

[29] Pozar, D. M. (2009). *Microwave engineering*. John Wiley & Sons.

[30] Tutkur, E. L. M. I. N. (2014). Wideband Directional Couplers and Power Splitters. *Unpublished Master of Science Thesis, Chalmers University of Technology*.

[31] Wight, J. S., Chudobiak, W. J., &Makios, V. (1976). A microstrip and stripline crossover structure (letters). *IEEE Transactions on Microwave Theory and Techniques*, *24*(5), 270-270.

[32] Khan, O. U. (2006, November). Design of X-band 4× 4 Butler matrix for microstrip patch antenna array. In *TENCON 2006. 2006 IEEE Region 10 Conference* (pp. 1-4). IEEE..